Available online at www.sciencedirect.com
ScienceDirect
Comput. Methods Appl. Mech. Engrg. 372 (2020) 113441
Computer methods in applied mechanics and engineering
www.elsevier.com/locate/cma

Quadrature formulas based on spline quasi-interpolation for hypersingular integrals arising in IgA-SGBEM

Alessandra Aimi[a], Francesco Calabrò[b,*], Antonella Falini[c], Maria Lucia Sampoli[d], Alessandra Sestini[e]

[a] *Department of Mathematical, Physical and Computer Science, University of Parma, Italy*
[b] *Department of Mathematics and Applications "R. Caccioppoli", University of Napoli "Federico II", Italy*
[c] *Department of Computer Science, University of Bari "Aldo Moro", Italy*
[d] *Department of Information Engineering and Mathematics, University of Siena, Italy*
[e] *Department of Mathematics and Computer Science, University of Firenze, Italy*

Received 29 June 2020; received in revised form 10 September 2020; accepted 10 September 2020
Available online xxxx

Abstract

In this paper, we study the construction of quadrature rules for the approximation of hypersingular integrals that occur when 2D Neumann or mixed Laplace problems are numerically solved using Boundary Element Methods. In particular the Galerkin discretization is considered within the Isogeometric Analysis setting and spline quasi-interpolation is applied to approximate integrand factors, then integrals are evaluated via recurrence relations. Convergence results of the proposed quadrature rules are given, with respect to both smooth and non smooth integrands. Numerical tests confirm the behavior predicted by the analysis. Finally, several numerical experiments related to the application of the quadrature rules to both exterior and interior differential problems are presented.

Keywords: Isogeometric analysis; Boundary element method; Quadrature formulas; Quasi-interpolation; Hypersingular integrals

1. Introduction

Boundary Element Methods (BEMs) have nowadays reached a high level of maturity [1]. The main advantages of BEMs compared with domain methods like Finite Element Method (FEM) or Finite Difference Method (FDM) are the dimensionality reduction and the implicit fulfillment of radiation condition at infinity for problems defined on unbounded domains. If a fundamental solution of the differential operator at hand is known in exact or approximated form, BEMs are employed to numerically solve Boundary Integral Equations (BIEs) where only information on the boundaries are used. This approach can be applied to elliptic, parabolic or hyperbolic partial differential equations (PDEs) modeling physical, engineering and recently also financial problems, see e.g. [2–6] for some current studies and applications.

* Corresponding author.
E-mail addresses: alessandra.aimi@unipr.it (A. Aimi), francesco.calabro@unina.it (F. Calabrò), antonella.falini@uniba.it (A. Falini), marialucia.sampoli@unisi.it (M.L. Sampoli), alessandra.sestini@unifi.it (A. Sestini).

https://doi.org/10.1016/j.cma.2020.113441
0045-7825/

Very different techniques are currently employed for the numerical solution of the arising BIEs. The first choice is between collocation and Galerkin: in both cases, the methods are written via some integrals in space variables with singular kernels, and the discrete counterpart is characterized by full matrices. Since BEMs first appearance, see e.g. [7], much effort has been devoted to the introduction of efficient integration schemes: we recall, for instance, analytical, semi-analytical and numerical techniques developed in the eighties and nineties for an accurate evaluation of weakly, strongly and hypersingular integrals related to elliptic problems, see e.g. [8] and references therein.

Also, the choice of the discrete space can be changed: the advent of Isogeometric Analysis (IgA) [9], initially confined only to FEM, in the last decade has brought also a renewed interest in BEMs [10–12]. In the IgA paradigm, the boundaries of the computational domains are represented in parametric form as Non-Uniform Rational B-Splines (NURBS), since this is the standard representation in CAD systems. Ad hoc quadratures are developed for IgA-Galerkin FEM, see the review in [13]. In IgA, the same representation is employed to define shape basis functions for the expression of the BIE approximate solution. This type of approach allows us to deal with functional spaces more regular and more flexible than those used by traditional schemes. This can be achieved by using spline functions which can have also different regularity at different inter-elements.

The IgA-BEM approach has given promising results in the numerical solution of several problems, ranging from acoustic to potential flow, elastostatic, steady incompressible flow. Collocation IgA-BEM has been applied to many different two- and three-dimensional problems, see [14,15] and references therein. Recently, also Galerkin conformal approximation [16] in IgA-BEM has been employed for three-dimensional problems [17–21]: in these contributions, reformulations are introduced to avoid the evaluation of hypersingular integrals. The present paper deals with the analysis of new quadrature rules for hypersingular integrals in two-dimensional problems. Indeed this feature still poses open questions related to efficiency and reliability [22–24].

In [25] one of the first numerical studies of Isogeometric Symmetric Galerkin BEM (IgA-SGBEM) for 2D elliptic problems has been conducted, highlighting the superiority of B-spline basis over classical Lagrangian basis involved in the standard case, in terms of achieved accuracy per used degrees of freedom. Moreover, in recent studies conducted by the same research group of the authors of the present paper, different innovative strategies for the evaluation of weakly singular integrals in 2D IgA-SGBEM Dirichlet Laplace problems have been introduced, giving remarkable computational advantages, see [26–28]. These are the results where the present paper starts from.

The aim of the current contribution is to complete the previous studies by introducing new quadrature rules for hypersingular integrals. For the proposed schemes we produce rigorous proofs of their convergence behavior, even when non-maximal smoothness is assumed. The new rules are then used to consider the discretization of 2D elliptic problems with pure Neumann or mixed boundary conditions and open the possibility to extend the techniques to more complex applications. The rigorous analysis gives insight about the important role played by the smoothness properties of the integrand and the singularity type of the kernel in order to derive convergence properties of the discrete BIEs. Note that, as done in other IgA papers, see e.g. [29,30], we always define our discretization space as a polynomial spline space even if the proposed approach could be generalized to NURBS discretization spaces. More precisely, our discretization space is (a possible h-refinement of) the spline space spanned by the B-splines used to describe the geometry in general NURBS form, in agreement to the more relaxed IgA paradigm, considering that, "for the essence of isogeometric analysis [...], what is needed is that the space describing the geometry and the one describing the solution share the same mesh" [31].

The approach of considering directly hypersingular BIEs, whose related integrals have to be understood in Hadamard Finite Part (HFP) sense, dates back to [32,33] and it was employed, on the basis of efficient quadrature rules for HFP integrals, as an alternative to the regularization of such integrals [34]. Here, we will consider the first approach in order to compare the innovative quadrature technique tailored for IgA with those used in the past and born in a Lagrangian basis context, as already mentioned. The new quadrature schemes can handle hypersingularities of order $O(r^{-k})$, $k \geq 2$ for $r \to 0$, and do not need any regularization of the kernel. We remark that our approach is alternative to the sinh transformation one, that is related to the reformulation of the BIEs in order to avoid the explicit evaluation of singular terms [20,35,36], and also to the construction of adaptive quadratures, as done in [28,37]. Moreover, even if here considered only in the context of 2D Laplace model problems, these quadrature rules can also be applied to BIEs coming from other 2D elliptic problems, such as Helmholtz or linear elasticity problems, having the same type of singularities.

The strategy here considered for the hypersingular quadrature relies on the spline product formula [38] and on spline quasi-interpolation, which is a very general and efficient approximation methodology, see e.g. [39] for an

introduction, having several other applications, for example in Dirichlet boundary data approximation of interest in IgA-FEM [40]. In particular, the proposed quadrature rules for hypersingular integrals are based on a variant of the Hermite spline quasi-interpolation approach introduced in [41], which requires just function information at the spline knots, see also [42]. Here the application to hypersingular integrals is analyzed, requiring the preliminary analytic computation of hypersingular specific basic integrals. Convergence results are given, developing the study for the first time also for functions not having maximal smoothness in the integration domain. The use of the presented quadratures in the IgA-BEM context allows us to adopt the faster basis-by-basis assembly procedure instead of the traditional element-by-element one, and here for the first time, such approach is applied also to problems with Neumann or mixed boundary conditions. Even if the proposed rules can be used also in the simpler framework of collocation IgA-BEM, in the present work we investigate their application to Galerkin IgA-BEM. In such setting the hypersingular kernel appears in the BIEs stemming from either exterior Neumann problems or mixed interior ones.

We conclude this introduction observing that, in particular in 3D simulations, fast methods for BEMs are mandatory to allow their coupling with FEMs and recently they have been applied also into the IgA context [19,43,44]. Even if we do not consider here such application, we believe that combining our quadrature rules with them could be of interest for the approximation of the near field integral contributions, provided that successive mesh elements forming the support of a basis function are clustered together for the integration.

The paper is organized as follows. In Section 2 we give our motivations for developing new efficient quadrature rules for hypersingular integrals, in particular with an integrand containing a B-spline factor and in Section 3 we detail IgA-SGBEM discretization. Then the adopted quasi-interpolation approach is summarized in Section 4, while in Section 5 we present the new quadrature formulas for hypersingular integrals, along with the analysis of their convergence behavior. Several numerical examples aimed to show their robustness and good performance in the context of IgA-SGBEM are discussed in Section 6. Finally Section 7 gives some concluding comments and some prospective on future studies.

2. Motivation

In this work we focus on the approximation of hypersingular integrals occurring in the Galerkin IgA-BEM numerical treatment of interior and exterior 2D Laplace model problems with mixed or pure Neumann boundary conditions. For the sake of completeness, in this section we introduce their boundary integral formulation and SGBEM discretization.

The geometries taken into account are bounded domains $\Omega \subset \mathbb{R}^2$ (not necessarily simply connected) with smooth boundaries or unbounded regions external to open arcs without self-intersections. In the first case, the domain boundary $\partial\Omega$ is assumed sufficiently regular and such that $\partial\Omega = \bar{\Gamma}_1 \cup \bar{\Gamma}_2$, where Γ_1 and Γ_2 are open disjoint subsets of $\partial\Omega$ and $\Gamma_1 \neq \emptyset$. We consider the following mixed boundary value problem (BVP) for the Laplace equation:

$$\begin{cases} \Delta u = 0 & \text{in } \Omega\,, \\ u = u^* & \text{on } \Gamma_1\,, \\ q := \frac{\partial u}{\partial \mathbf{n}} = q^* & \text{on } \Gamma_2\,, \end{cases} \tag{1}$$

where u^*, q^* are given data and $\frac{\partial}{\partial \mathbf{n}}$ denotes the derivative with respect to the outer unit normal $\mathbf{n}$ to $\partial\Omega$, while we denote by $\mathbf{n_x}$, $\mathbf{n_y}$ the components of the same vector with respect to x and y coordinate, respectively. The symmetric boundary integral formulation of problem (1) is based on the use of the so-called BIE quartet, whose properties are studied in [45]:

$$\begin{aligned} Vq(\mathbf{x}) &:= \int_{\partial\Omega} U(\mathbf{x},\mathbf{y})\, q(\mathbf{y}) \mathrm{d}\gamma_{\mathbf{y}}\,, \qquad & Ku(\mathbf{x}) &:= \int_{\partial\Omega} \frac{\partial U}{\partial \mathbf{n_y}}(\mathbf{x},\mathbf{y})\, u(\mathbf{y}) \mathrm{d}\gamma_{\mathbf{y}}\,, \\ K'q(\mathbf{x}) &:= \int_{\partial\Omega} \frac{\partial U}{\partial \mathbf{n_x}}(\mathbf{x},\mathbf{y})\, q(\mathbf{y}) \mathrm{d}\gamma_{\mathbf{y}}\,, & Du(\mathbf{x}) &:= \int_{\partial\Omega} \frac{\partial^2 U}{\partial \mathbf{n_x} \partial \mathbf{n_y}}(\mathbf{x},\mathbf{y})\, u(\mathbf{y}) \mathrm{d}\gamma_{\mathbf{y}}\,, \end{aligned} \tag{2}$$

where we denote the fundamental solution of the 2D Laplace operator by

$$U(\mathbf{x},\mathbf{y}) := -\frac{1}{2\pi} \ln r\,, \quad \text{with } \mathbf{r} := \mathbf{y} - \mathbf{x},\ r := \|\mathbf{r}\|_2$$

and

$$\frac{\partial U}{\partial \mathbf{n}_\mathbf{y}}(\mathbf{x},\mathbf{y}) = \frac{1}{2\pi}\frac{\mathbf{r}\cdot\mathbf{n}_\mathbf{y}}{r^2}, \quad \frac{\partial U}{\partial \mathbf{n}_\mathbf{x}}(\mathbf{x},\mathbf{y}) = -\frac{1}{2\pi}\frac{\mathbf{r}\cdot\mathbf{n}_\mathbf{x}}{r^2},$$

$$\frac{\partial^2 U}{\partial \mathbf{n}_\mathbf{x}\partial \mathbf{n}_\mathbf{y}}(\mathbf{x},\mathbf{y}) = -\frac{1}{2\pi}\left(\frac{\mathbf{n}_\mathbf{x}\cdot\mathbf{n}_\mathbf{y}}{r^2} - 2\frac{\mathbf{r}\cdot\mathbf{n}_\mathbf{x}\,\mathbf{r}\cdot\mathbf{n}_\mathbf{y}}{r^4}\right). \tag{3}$$

The operator K' is the adjoint of K with respect to the natural duality $\langle\cdot,\cdot\rangle$ between $H^{1/2}(\partial\Omega)$ and its dual $H^{-1/2}(\partial\Omega)$, which for sufficiently smooth functions coincides with the usual scalar product in $L^2(\partial\Omega)$ and V, D are self-adjoint operators, see [46]. Note that U is weakly singular for $r \to 0$; K and K' kernels behave as $O(r^{-1})$, while the kernel in D as $O(r^{-2})$, for $r \to 0$.

Now, using the assigned boundary data, the differential problem is written as a system of two BIEs in the unknown u on Γ_2 and q on Γ_1 of the following form:

$$\begin{bmatrix} V_{11} & -K_{12} \\ -K'_{21} & D_{22} \end{bmatrix}\begin{bmatrix} q \\ u \end{bmatrix} = \begin{bmatrix} f_1 \\ f_2 \end{bmatrix}, \tag{4}$$

where the boundary integral operators subscripts jk mean evaluation over Γ_j and integration over Γ_k and where

$$\begin{bmatrix} f_1 \\ f_2 \end{bmatrix} := \begin{bmatrix} -V_{12} & \frac{1}{2}I + K_{11} \\ -\frac{1}{2}I + K'_{22} & -D_{21} \end{bmatrix}\begin{bmatrix} q^* \\ u^* \end{bmatrix}.$$

Then the symmetric weak formulation of (4) reads: *given* $u^* \in H^{1/2}(\Gamma_1)$ and $q^* \in H^{-1/2}(\Gamma_2)$, *find* $[q,u] \in H^{-1/2}(\Gamma_1)\times H_0^{1/2}(\Gamma_2)$ *such that* $\forall\,[p,v] \in H^{-1/2}(\Gamma_1)\times H_0^{1/2}(\Gamma_2)$:

$$\left\langle \begin{bmatrix} V_{11} & -K_{12} \\ -K'_{21} & D_{22} \end{bmatrix}\begin{bmatrix} q \\ u \end{bmatrix}, \begin{bmatrix} p \\ v \end{bmatrix}\right\rangle = \left\langle \begin{bmatrix} f_1 \\ f_2 \end{bmatrix}, \begin{bmatrix} p \\ v \end{bmatrix}\right\rangle. \tag{5}$$

After recovering the missing Cauchy data on $\partial\Omega$, the solution of (1) can be evaluated from the integral representation formula:

$$u(\mathbf{x}) = Vq(\mathbf{x}) - Ku(\mathbf{x}), \quad \mathbf{x} \in \Omega.$$

The case of $\Gamma_1 = \emptyset$, $\Gamma_2 = \partial\Omega$, i.e. of a pure Neumann datum, is also dealt with. In this case the compatibility condition $\int_{\partial\Omega} q^*(\mathbf{x})\mathrm{d}\gamma_\mathbf{x} = 0$ is required and the weak BIE system (5) collapses to only one equation,

$$\langle Du, v\rangle = \langle(-\frac{1}{2}I + K')q^*, v\rangle, \tag{6}$$

which admits solution up to an additive constant that can be fixed imposing the further constraint $\int_{\partial\Omega} u(\mathbf{x})\mathrm{d}\gamma_\mathbf{x} = 0$, as discussed in [47].

The third model problem here analyzed, involving again evaluations of hypersingular integrals, is a classic case where BEMs are preferred to FEMs: a problem in an infinite domain outside a bounded obstacle. Still denoting with $\partial\Omega$ an open arc in the plane, we consider:

$$\begin{cases} \Delta u = 0 & \text{in } \mathbb{R}^2 \setminus \partial\Omega, \\ q = q^* & \text{on } \partial\Omega, \\ u = O(\|\mathbf{x}\|_2^{-1}), & \|\mathbf{x}\| \to \infty. \end{cases} \tag{7}$$

Choosing an indirect approach [1,48], the BIE coming from the boundary integral reformulation of (7) reads:

$$D\,\varphi(\mathbf{x}) = q^*(\mathbf{x}), \quad \mathbf{x} \in \partial\Omega, \tag{8}$$

with the unknown density function φ over $\partial\Omega$.

The price for the simplification of the indirect approach is that the BIE solution does not give the missing Cauchy data on the boundary, but just the density function appearing in the chosen double layer integral representation formula of the PDE solution:

$$u(\mathbf{x}) = K\varphi(\mathbf{x}), \quad \mathbf{x} \in \Omega.$$

Boundary integral problem (8) can be set in the weak form [1]: *given* $q^* \in H^{-1/2}(\partial\Omega)$, *find* $\varphi \in H_0^{1/2}(\partial\Omega)$*:*

$$\langle D\,\varphi, \psi\rangle = \langle q^*, \psi\rangle, \quad \forall\,\psi \in H_0^{1/2}(\partial\Omega). \tag{9}$$

As already mentioned, the discretization approach adopted here is the Galerkin projection which for brevity is reported just referring to the mixed problem in (5). Denoting with $V_h^{(i)}, i = 1, 2$ two finite dimensional subspaces respectively of $H^{-1/2}(\Gamma_1)$ and $H_0^{1/2}(\Gamma_2)$, where h is a discretization parameter going to zero when the dimension of V_h increases, the considered discrete problem can be formulated as follows: *given* $u^* \in H^{1/2}(\Gamma_1)$ *and* $q^* \in H^{-1/2}(\Gamma_2)$*, find* $[q_h, u_h] \in V_h^{(1)} \times V_h^{(2)}$ *such that* $\forall\, [p_h, v_h] \in V_h^{(1)} \times V_h^{(2)}$*:*

$$\left\langle \begin{bmatrix} V_{11} & -K_{12} \\ -K_{21}' & D_{22} \end{bmatrix} \begin{bmatrix} q_h \\ u_h \end{bmatrix}, \begin{bmatrix} p_h \\ v_h \end{bmatrix} \right\rangle = \left\langle \begin{bmatrix} f_1 \\ f_2 \end{bmatrix}, \begin{bmatrix} p_h \\ v_h \end{bmatrix} \right\rangle. \tag{10}$$

3. IgA-SGBEM approach

In order to specify the discrete problem (10) in the IgA-SGBEM context, let us introduce some notation for the mathematical description of the boundary and of the discretization spaces $V_h^{(i)}, i = 1, 2$. Concerning the boundary, we assume that each curve $\bar{\Gamma}_i, i = 1, 2$ is parametrically defined as the image of a regular invertible function $\mathbf{F}_i : [a_i\,,\, b_i] \to \mathbb{R}^2$ given in NURBS form,[1]

$$\mathbf{F}_i(s) := \sum_{j=1}^{N_i} \mathbf{Q}_j^{(i)}\, R_{j,d_i}^{(i)}(s)\,, \quad s \in [a_i\,,\, b_i]\,, \quad i = 1, 2\,, \tag{11}$$

where the $\mathbf{Q}_j^{(i)}$, $j = 1, \ldots, N_i$, are ordered control points assigned in the plane, defining the shape of Γ_i and

$$R_{j,d_i}^{(i)}(s) := \frac{w_j^{(i)}\; B_{j,d_i}^{(i)}(s)}{\sum_{k=1}^{N_i} w_k^{(i)}\; B_{k,d_i}^{(i)}(s)} \tag{12}$$

with $\{B_{j,d_i}^{(i)}.j = 1, \ldots, N_i\}$ denoting a B-spline basis spanning a space $\mathbb{S}_i$ of piecewise d_i-degree polynomials with respect to an assigned set Δ_i of breakpoints in $[a_i, b_i]$. The weights $w_k^{(i)}, k = 1, \ldots, N_i$ appearing in (12) are positive coefficients which can be useful to obtain further control on the shape of the parametric curve defined in (11). As well known, each $B_{j,d_i}^{(i)}$ and consequently each $R_{j,d_i}^{(i)}$ has local support, which will be denoted in the following by $D_j^{(i)}$ and it is clear that $R_{j,d_i}^{(i)} = B_{j,d_i}^{(i)}\ \forall j$ when the weights are all equal to a common constant value.

Remark 1. We note that, if the boundary is originally given with just one parametric NURBS representation, by using repeated knot insertion, see e.g. [49], two separate representations for Γ_1 and Γ_2 can always be easily obtained. Such algorithm can be used also for dealing with the more involved situation of Dirichlet and/or Neumann boundary conditions assigned on disjoint curves. For the sake of simplicity here we do not consider such case.

From here on, in order to simplify the notation, we omit the superscript (i) (or the subscript i) when it is not strictly necessary and/or clear from the context.

We start observing that the dimension N of the spline space $\mathbb{S}$, as well as the regularity required at each inner breakpoint, can be a priori established. In any case the definition of the B-spline basis needs the preliminary introduction of the extended knot vector $T := \{t_1, \ldots, t_d, t_{d+1}, \ldots, t_{N+1}, t_{N+2}, \ldots, t_{N+d+1}\}$, where $t_{d+1} = a$, $t_{N+1} = b$, and $t_1 \le \cdots \le t_{N+d+1}$. Each knot t_i, $i = d+2, \ldots, N$, is a possibly repeated occurrence of an inner breakpoint, while the first and last d knots in T are auxiliary knots characterizing a specific B-spline basis. The regularity at a certain inner breakpoint in Δ of a general function in $\mathbb{S}$ is fully specified by prescribing the breakpoint multiplicity (an integer between 1 and $d+1$) in T. In particular since we want Γ to be at least a regular curve, such multiplicities are required to be all $\le d-1$, which guarantees that $\mathbf{F} \in C^1[a\,,\, b]$. Extended knot vectors with *multiple* or *periodic* auxiliary knots are the more commonly adopted strategies for completing the definition of T, see e.g. [50]. We adopt the standard way to represent closed curves used in Computer Aided Geometric Design (CAGD) that relies on periodic extended knot vectors and on fixing the last d control points as an ordered repetition of the first d ones. This clearly means that in practice the dimension of the considered spline space $\mathbb{S}$ is $N - d$.

In the relaxed IgA setting we are here adopting, the discretization space V_h is defined as a possible enlargement of $\mathbb{S}$, where h denotes the maximal spacing between breakpoints of (the enlargement of) $\mathbb{S}$. When Γ is an open arc, we define $V_h := span\{\hat{B}_{1,d}, \ldots, \hat{B}_{N,d}\}$, where

$$\hat{B}_j(\mathbf{x}) := B_{j,d}(\mathbf{F}^{-1}(\mathbf{x}))\,, \quad \mathbf{x} \in \Gamma\,, \qquad j = 1, \ldots, N\,. \tag{13}$$

[1] When $\bar{\Gamma}_i$ is a closed curve, clearly we assume $\mathbf{F}_i(a_i) = \mathbf{F}_i(b_i)$.

When Γ is a closed curve, the dimension of V_h must be equal to $N-d$. Thus we fix V_h as

$$V_h := span\{\hat{B}_{1,d}, \ldots, \hat{B}_{N-d,d}\},$$

where $\hat{B}_{j,d},\ j = d+1, \ldots, N-d$ are defined as in (13); while we have

$$\hat{B}_{j,d}(\mathbf{x}) := B^{(c)}_{j,d}(\mathbf{F}^{-1}(\mathbf{x})), \quad \mathbf{x} \in \Gamma, \qquad j = 1, \ldots, d,$$

with

$$B^{(c)}_{j,d}(t) := \begin{cases} B_{j,d}(t) & \text{if } t \in I \cap [t_j, t_{j+d+1}], \\ B_{N-d+j,d}(t) & \text{if } t \in I \cap [t_{N-d+j}, t_{N+j+1}], \\ 0 & \text{otherwise}. \end{cases}$$

To simplify the notation, in the sequel, when Γ is closed we omit the superscript (c) to denote the first d cyclic basis elements.

In order to obtain richer spaces, V_h can be enlarged either performing a *d--refinement* or a *h--refinement*, by using the robust degree-elevation or knot-insertion algorithms, see e.g. [49]. In the following we assume that the possible enlargement is obtained by inserting in the knot vector T new breakpoints with unit multiplicity.

The algebraic reformulation of the IgA-SGBEM scheme leads to a block linear system of equations, whose unknowns represent the coefficients of the BIE approximate solution with respect to the chosen basis, see e.g. [46]. In more detail, denoting such a solution with

$$q_h(\mathbf{x}) := \sum_{j=1}^{N^{(1)}_{DoF}} \alpha^{(1)}_j \hat{B}^{(1)}_{j,d_1-1}(\mathbf{x}) \quad u_h(\mathbf{x}) := \sum_{j=1}^{N^{(2)}_{DoF}} \alpha^{(2)}_j \hat{B}^{(2)}_{j,d_2}(\mathbf{x}), \tag{14}$$

with $N^{(i)}_{DoF} := dim(V^{(i)}_h),\ i = 1, 2$ the resulting linear system has size $N_{DoF} := N^{(1)}_{DoF} + N^{(2)}_{DoF}$ and it is referred to as follows,

$$\begin{pmatrix} A_{11} & A_{12} \\ A_{21} & A_{22} \end{pmatrix} \begin{pmatrix} \boldsymbol{\alpha}^{(1)} \\ \boldsymbol{\alpha}^{(2)} \end{pmatrix} = \begin{pmatrix} \boldsymbol{\beta}^{(1)} \\ \boldsymbol{\beta}^{(2)} \end{pmatrix}, \tag{15}$$

where $\boldsymbol{\alpha}^{(i)} := (\alpha^{(i)}_1, \ldots, \alpha^{(i)}_{N^{(i)}_{DoF}})^T,\ i = 1, 2$ are the unknown vectors, the coefficient matrix is non-singular and symmetric [8], and $\boldsymbol{\beta}^{(i)} := (\beta^{(i)}_1, \ldots, \beta^{(i)}_{N^{(i)}_{DoF}})^T,\ i = 1, 2$ are the vectors defining the right-hand side which depends on the given Cauchy data.

In particular, the entries of the blocks of the matrix in (15) are given by the following double integrals:

$$(A_{11})_{j,k} := \int_{\Gamma_1} \hat{B}^{(1)}_{j,d_1-1}(\mathbf{x}) \int_{\Gamma_1} U(\mathbf{x}, \mathbf{y}) \hat{B}^{(1)}_{k,d_1-1}(\mathbf{y})\, d\gamma_{\mathbf{y}} d\gamma_{\mathbf{x}}, \tag{16}$$

$$(A_{12})_{j,k} = (A_{21})_{k,j} := -\int_{\Gamma_1} \hat{B}^{(1)}_{j,d_1-1}(\mathbf{x}) \int_{\Gamma_2} \frac{\partial U}{\partial \mathbf{n}_{\mathbf{y}}}(\mathbf{x}, \mathbf{y}) \hat{B}^{(2)}_{k,d_2}(\mathbf{y})\, d\gamma_{\mathbf{y}} d\gamma_{\mathbf{x}}, \tag{17}$$

$$(A_{22})_{j,k} := \int_{\Gamma_2} \hat{B}^{(2)}_{j,d_2}(\mathbf{x}) \int_{\Gamma_2} \frac{\partial^2 U}{\partial \mathbf{n}_{\mathbf{x}} \partial \mathbf{n}_{\mathbf{y}}}(\mathbf{x}, \mathbf{y}) \hat{B}^{(2)}_{k,d_2}(\mathbf{y})\, d\gamma_{\mathbf{y}} d\gamma_{\mathbf{x}}. \tag{18}$$

We observe that, when the supports of the involved B-splines overlap, the inner integrals defining the corresponding entries of A_{11} are weakly singular while those in (18) are hypersingular. On the other hand, the entries of A_{12} are never singular, except in $\bar{\Gamma}_1 \cap \bar{\Gamma}_2 \neq \emptyset$ (i.e. when the supports of $\hat{B}^{(1)}_{j,d_1-1}$ and $\hat{B}^{(2)}_{k,d_2}$ are consecutive, and joining at a contact point in $\bar{\Gamma}_1 \cap \bar{\Gamma}_2$); in such case the related kernel presents a strong singularity if the contact point is a corner, a weak singularity in case of a junction with Lyapunov continuity and no singularity in the case of a junction with C^2 regularity [51].

Regarding the right-hand side, it can be explicitly written as

$$\boldsymbol{\beta}^{(1)}_j := \frac{1}{2} \int_{\Gamma_1} \hat{B}^{(1)}_{j,d_1-1}(\mathbf{x}) u^*(\mathbf{x}) d\gamma_{\mathbf{x}} + \int_{\Gamma_1} \hat{B}^{(1)}_{j,d_1-1}(\mathbf{x}) \int_{\Gamma_1} \frac{\partial U}{\partial \mathbf{n}_{\mathbf{y}}}(\mathbf{x}, \mathbf{y})\, u^*(\mathbf{y})\, d\gamma_{\mathbf{y}} - \int_{\Gamma_1} \hat{B}^{(1)}_{j,d_1-1}(\mathbf{x}) \int_{\Gamma_2} U(\mathbf{x}, \mathbf{y})\, q^*(\mathbf{y})\, d\gamma_{\mathbf{y}} d\gamma_{\mathbf{x}}, \tag{19}$$

$$\boldsymbol{\beta}_j^{(2)} := -\frac{1}{2}\int_{\Gamma_2} \hat{B}^{(2)}_{j,d_2}(\mathbf{x}) q^*(\mathbf{x}) d\gamma_{\mathbf{x}} + \int_{\Gamma_2} \hat{B}^{(2)}_{j,d_2}(\mathbf{x}) \int_{\Gamma_2} \frac{\partial U}{\partial \mathbf{n}_{\mathbf{x}}}(\mathbf{x},\mathbf{y})\; q^*(\mathbf{y})\; d\gamma_{\mathbf{y}} - \int_{\Gamma_2} \hat{B}^{(2)}_{j,d_2}(\mathbf{x}) \int_{\Gamma_1} \frac{\partial^2 U}{\partial \mathbf{n}_{\mathbf{x}} \partial \mathbf{n}_{\mathbf{y}}}(\mathbf{x},\mathbf{y})\; u^*(\mathbf{y})\; d\gamma_{\mathbf{y}} d\gamma_{\mathbf{x}}\,. \tag{20}$$

The inner integrals in the right-hand side can be singular: in particular, in the second addend of (19) as well as of (20) for $r \to 0$ when $\mathbf{F}_i$ are less regular than $C^2([a_i, b_i])$, and in the third addend of (19) as well as of (20), but only if $\bar{\Gamma}_1 \cap \bar{\Gamma}_2 \neq \emptyset$ and the support of $\hat{B}^{(1)}_{j,d_1-1}\big(\hat{B}^{(2)}_{j,d_2}\big)$ starts or ends at a contact point between Γ_1 and Γ_2 (the first one being weakly and the second hypersingular). Since the focus of the present work is the numerical treatment of hypersingular integrals, in the next subsection we analyze in detail how the integrals in (18) and in the third addend of (20) are suitably expressed in the parametric setting. For the sake of simplicity, the case of corner points in $\bar{\Gamma}_1 \cap \bar{\Gamma}_2$ is not considered.

For all the other integrals necessary to complete the assembly of the coefficient matrix and the right-hand side of the linear system (15), we refer to [28] and [26].

3.1. Hypersingular integrals in IgA-SGBEM

Let us first focus on the integrals in (18), in particular referring to the case of Γ_2 being an open curve. Since both the inner and outer integration are done in Γ_2, for brevity we omit the subscript or the superscript used to distinguish between Γ_1 and Γ_2. Setting

$$s := \mathbf{F}^{-1}(\mathbf{x}),\;\; \mathbf{x} \in \Gamma \qquad t := \mathbf{F}^{-1}(\mathbf{y}),\;\; \mathbf{y} \in \Gamma,$$

we have $(A_{22})_{j,k} = I^{(j,k)}$, where

$$I^{(j,k)} := \int_{D_j} B_{j,d}(s)\, J(s) \int_{D_k} \frac{\partial^2 U}{\partial \mathbf{n}_{\mathbf{x}} \partial \mathbf{n}_{\mathbf{y}}}(\mathbf{F}(s),\mathbf{F}(t))\;\; B_{k,d}(t)\, J(t)\, dt\, ds, \tag{21}$$

with $J(\cdot) := \|\mathbf{F}'(\cdot)\|_2$ denoting the parametric speed associated with Γ.

Now, with some computations we can obtain

$$\frac{\mathbf{n}_{\mathbf{x}} \cdot \mathbf{n}_{\mathbf{y}}}{r^2} = \frac{1}{J(s)\; J(t)}\; \frac{\mathbf{F}'(s) \cdot \mathbf{F}'(t)}{\|\mathbf{F}(s) - \mathbf{F}(t)\|_2^2},$$

$$\frac{\mathbf{r} \cdot \mathbf{n}_{\mathbf{x}}\; \mathbf{r} \cdot \mathbf{n}_{\mathbf{y}}}{r^4} = \frac{1}{J(s)\; J(t)}\; \frac{\big(\big(\mathbf{F}(s) - \mathbf{F}(t)\big) \times \mathbf{F}'(s)\big)\big(\big(\mathbf{F}(s) - \mathbf{F}(t)\big) \times \mathbf{F}'(t)\big)}{\|\mathbf{F}(s) - \mathbf{F}(t)\|_2^4},$$

where the symbol $\times$ denotes the cross product between 2D vectors ($\mathbf{v} \times \mathbf{w} = v_1 w_2 - v_2 w_1$). Then, considering (3), these relations allow us to write the following formula,

$$\frac{\partial^2 U}{\partial \mathbf{n}_{\mathbf{x}} \partial \mathbf{n}_{\mathbf{y}}}(\mathbf{F}(s),\mathbf{F}(t)) = -\frac{1}{2\pi}\; \frac{1}{J(s)\; J(t)} \Big(\mathcal{K}(s,t)\; P(s,t) - \hat{\mathcal{K}}(s,t)\Big),$$

where

$$P(s,t) := \frac{(s-t)^2}{\|\mathbf{F}(s) - \mathbf{F}(t)\|_2^2}\; \big(\mathbf{F}'(s) \cdot \mathbf{F}'(t)\big), \tag{22}$$

and

$$\mathcal{K}(s,t) := \frac{1}{(s-t)^2}, \tag{23}$$

$$\hat{\mathcal{K}}(s,t) := 2\, \overline{\mathcal{K}}(s,t)\, \overline{\mathcal{K}}(t,s), \qquad \overline{\mathcal{K}}(s,t) := \frac{\big(\mathbf{F}(s) - \mathbf{F}(t)\big) \times \mathbf{F}'(s)}{\|\mathbf{F}(s) - \mathbf{F}(t)\|_2^2}.$$

Note that $\mathcal{K}$ does not depend on the geometry and $\hat{\mathcal{K}}$ is not singular if $\mathbf{F}$ is C^2 smooth, since in such a case we have

$$\lim_{t \to s} \overline{\mathcal{K}}(s,t) = \frac{\mathbf{F}'(s) \times \mathbf{F}''(s)}{J^2(s)}\,. \tag{24}$$

Also, the function P is not singular, as proved in Proposition 1, where some important considerations about its smoothness are derived. Concluding, formula (21) can be rewritten as follows

$$I^{(j,k)} = \frac{1}{2\pi} \int_{D_j} B_{j,d}(s) \int_{D_k} \hat{\mathcal{K}}(s,t)\ B_{k,d}(t)\, dt\, ds - \frac{1}{2\pi} \int_{D_j} B_{j,d}(s) \int_{D_k} \mathcal{K}(s,t)\, P(s,t)\ B_{k,d}(t)\, dt\, ds\,. \tag{25}$$

Note that when $\bar{\mathcal{K}}$ and P have to be computed for the quadrature at a parameter point (t,s) with t suitably near to s, their limit value reported in (24) and in Proposition (1) below, respectively, is used in the implementation. When Γ is a closed curve, that is $F(a) = F(b)$, the same limit value is used also when both s and t nearly approach either a or b, adopting a shift technique for the treatment of such circumstance.

Concerning the algebraic manipulation developed above to transform formula (21) into (25), we observe that it can be extended to other types of kernels with the same hypersingularity order. The key point in any case is to rewrite the kernel in the form $\mathcal{K}(s,t)\tilde{P}(s,t)+\tilde{\mathcal{K}}(s,t)$, with $\mathcal{K}$ defined as in (23), $\tilde{\mathcal{K}}$ denoting a suitable non singular kernel and $\tilde{P}$ being the product between the factor $\frac{(s-t)^2}{\|\mathbf{F}(s)-\mathbf{F}(t)\|_2^2}$ also appearing in formula (22) and another suitable sufficiently smooth function.

The inner integral in the second addend on the right of (25) is hypersingular when $D_j \cap D_k \neq \emptyset$ and can be considered a particular case of the following general one, which is formulated on the reference integration interval $[0\,,\,1]$,

$$I_{w,m}[g,\sigma] := \Xint-_0^1 w(\tau)\frac{g(\tau)}{(\tau-\sigma)^{m+1}}\, d\tau\,, \quad 0 \le \sigma \le 1\,,\ m \in \mathbb{N}\,,\ m \ge 1\,, \tag{26}$$

where w is a weight function possibly containing integrable endpoint singularities and g is a sufficiently smooth function (see the beginning of Section 5 for more details on the required smoothness). Referring to [52] for an introduction which covers also the case of end hypersingularities, we first note that, in the IgA-SGBEM setting here considered, we deal just with $m = 1$ and with w at least $C^1[0\,,\,1]$. Indeed, considering the linear mapping $\mathcal{L}_k : D_k \to [0\,,\,1]$, that is setting $\tau = \mathcal{L}_k(t) = (t - t_k)/\ell_k$, with $\ell_k := |D_k| := t_{k+d+1} - t_k$, the inner integral in the second addend of (25) becomes the integral in (26) with $m = 1$, where,

$$g(\tau) = g_\sigma^{(k)}(\tau) = \frac{1}{\ell_k^m} P(t_k + \ell_k\sigma, t_k + \ell_k\tau)\,, \quad w(\tau) = B(\tau) := B_{k,d}(t_k + \ell_k\tau)\,, \tag{27}$$

and $\sigma := (s - t_k)/\ell_k$. Note that the singularity is active, i.e., σ belongs to $[0\,,\,1]$, if and only if s belongs to the support of $B_{k,d}$. Note also that the weight function $w = B$ is a B-spline of degree d with support equal to $[0\,,\,1]$ and active knots with the same distribution of the active knots of $B_{k,d}$. Furthermore B belongs at least to $C^1[0\,,\,1]$ because of the assumptions on the adopted refinement strategy and since the original inner knots in T have at most multiplicities $d - 1$. In order to study the smoothness of $g_\sigma^{(k)}$, we firstly introduce the following proposition.

Proposition 1. *For the function P defined in (22) the following limits hold,*

$$\lim_{t\to s} P(s,t) = \lim_{s\to t} P(s,t) = 1\,, \qquad \lim_{t\to s} \frac{\partial P}{\partial t}(s,t) = \lim_{s\to t} \frac{\partial P}{\partial s}(s,t) = 0.$$

Proof. Since P is fully symmetric with respect to its arguments, we can focus just on the limits for $t \to s$. Let us firstly consider s different from any breakpoint of $\mathbf{F}$. Then, using the Taylor expansion of $\mathbf{F}(t)$ at $t = s$, we can write

$$\frac{\mathbf{F}(t) - \mathbf{F}(s)}{t - s} = \mathbf{F}'(s) + \frac{1}{2}\mathbf{F}''(s)(t - s) + \frac{1}{6}\mathbf{F}'''(s)(t - s)^2 + O((t - s)^3).$$

This implies that

$$\left\| \frac{\mathbf{F}(t) - \mathbf{F}(s)}{t - s} \right\|_2^2 = \|\mathbf{F}'(s)\|_2^2 + \big(\mathbf{F}'(s) \cdot \mathbf{F}''(s)\big)(t - s) + \left[\frac{1}{3}\big(\mathbf{F}'(s) \cdot \mathbf{F}'''(s)\big) + \frac{1}{4}\|\mathbf{F}''(s)\|_2^2 \right] (t - s)^2 + O((t - s)^3)\,.$$

Since the zero and first order terms of this expansion are equal to the same order terms of the Taylor expansion of $\mathbf{F}'(s)\cdot\mathbf{F}'(t)$ at $t=s$, with some computation the statement of the theorem can be proved, considering that $P(s,t)$ is the ratio between $\mathbf{F}'(s)\cdot\mathbf{F}'(t)$ and $\|\frac{\mathbf{F}(t)-\mathbf{F}(s)}{t-s}\|_2^2$. When s is a breakpoint for $\mathbf{F}$, since the above steps can be repeated for the left and right limits, we arrive at the thesis as well. □

As a consequence of this proposition, we can say that (the continuous extension of) $g_\sigma^{(k)}$ is at least C^1 at $\tau=\sigma$, and can be even smoother when $s\notin T$. When s is a breakpoint for $\mathbf{F}$, it becomes at least C^2 at $\tau=\sigma$ provided the existence of the limit for $t\to s$ of the following function $\rho(t)$,

$$\rho(t) := \frac{1}{\|\mathbf{F}'(t)\|_2^2}\left[\frac{1}{3}\big(\mathbf{F}'(t)\cdot\mathbf{F}'''(t)\big)-\frac{1}{2}\|\mathbf{F}''(t)\|_2^2\right]. \tag{28}$$

Indeed, at any $s\notin T$ we have $\dfrac{\partial^2 P}{\partial t^2}(s,s)=\rho(s)$. Note that, since $\mathbf{F}$ is piecewise polynomial, C^1 and regular, ρ is continuous at any $s\notin T$. On the other hand, if s coincides with a breakpoint of $\mathbf{F}$ and $\lim\limits_{t\to s}\rho(t)$ exists, such limit is surely finite. Thus, when this is true at any breakpoint of $\mathbf{F}$, the function ρ admits a globally continuous extension and this ensures that for any k and any σ the continuous extension of the function $g_\sigma^{(k)}$ is at least C^2 at $\tau=\sigma$.

From a global point of view, we can only state that $g_\sigma^{(k)}\in C^R[0\,,\,1]$, where R denotes the difference between $d-1$ and the maximal multiplicities of the knots in T, with $R\geq 0$ for the given assumptions on the assayed multiplicities, although $g_\sigma^{(k)}$ could be globally even smoother if the control polygon associated to $\mathbf{F}$ has some specific configuration. However, Proposition 1 implies that at $\tau=\sigma$ we can be sure that $g_\sigma^{(k)}$ is always at least C^1.

Let us now consider $I^{(j,*)}$ which denotes the third addend in (20). As already mentioned, such integral becomes singular only when $\bar{\Gamma}_1\cap\bar{\Gamma}_2\neq\emptyset$ and the support of $B^{(2)}_{j,d_2}$ starts or ends at a point belonging to such intersection. Now setting

$$s := \mathbf{F}_2^{-1}(\mathbf{x}),\ \ \mathbf{x}\in\Gamma_2\,,\quad t := \mathbf{F}_1^{-1}(\mathbf{y}),\ \ \mathbf{y}\in\Gamma_1,$$

the same analysis done for $I^{(j,k)}$ can be applied, in order to write,

$$\begin{aligned} I^{(j,*)} \;=\; & -\frac{1}{2\pi}\int_{D_j^{(2)}} B^{(2)}_{j,d_2}(s)\int_{a_1}^{b_1}\hat{\mathcal{K}}(s,t)\;u^*(\mathbf{F}_1(t))\,dt\,ds\;+ \\ & \frac{1}{2\pi}\int_{D_j^{(2)}} B^{(2)}_{j,d_2}(s)\int_{a_1}^{b_1}\mathcal{K}(s,t)\,P(s,t)\;u^*(\mathbf{F}_1(t))\,dt\,ds\,. \end{aligned} \tag{29}$$

Using the substitution $\tau=(t-a_1)/\delta_1$, with $\delta_1:=b_1-a_1$, we arrive to an integral of the form (26), again with $m=1$ and where,

$$g(\tau)=g_\sigma(\tau)=\frac{1}{\delta_1^m}P(a_1+\delta_1\sigma,a_1+\delta_1\tau)\,u^*\big(\mathbf{F}_1(a_1+\delta_1\tau)\big)\,,\qquad w(\tau)\equiv 1\,, \tag{30}$$

having set in this case $\sigma:=(s-a_1)/\delta_1$ which can take only the values 0 or 1 when the singularity is active. Clearly in this case the regularity in $[0\,,\,1]$ of g defined in (30) depends not only on the regularity of the factor P but also on the regularity of the datum u^*.

The hypersingular quadrature formulas introduced in Section 5 are based on the general idea of approximating g in $[0\,,\,1]$ with low computational cost by using a spline function defined by quasi-interpolation. The adopted quasi-interpolation approach, introduced in [41], is briefly summarized in the next section.

4. Approximated Hermite Quasi-Interpolation schemes

Let us briefly summarize the Hermite spline Quasi Interpolation (QI) approach introduced in [41]. This approach requires function and function derivative values only at the spline knots and it was firstly introduced to define, with low computational cost, continuous approximations of the solution of 1D boundary value problems, starting from an available numerical solution. In particular, we consider the variant proposed in [42], which does not require derivative values, firstly used there for defining quadrature rules for regular integrals and more recently in [27], for dealing with weakly and strongly singular integrals.

For the sake of completeness we report here the main ideas of the basic Hermite QI scheme; then the differences of the considered variant are sketched. Without loss of generality we can consider functions defined on the interval

$[0\,,\,1]$. Given a function g, the goal is to construct an approximating spline S_g defined on a space $\mathbb{S}_{\boldsymbol{\theta},p}$ of degree p, $\mathbb{S}_{\boldsymbol{\theta},p} := \langle B^{(\boldsymbol{\theta})}_{-p,p}, \ldots, B^{(\boldsymbol{\theta})}_{n-1,p}\rangle$, where $B^{(\boldsymbol{\theta})}_{j,p}$, $j = -p, \ldots, n-1$, are the p-degree B-splines with respect to the extended knot vector $\boldsymbol{\theta} := \{\theta_{-p}, \ldots, \theta_{n+p}\}$, with $0 = \theta_{-p} = \cdots = \theta_0 < \cdots < \theta_n = \cdots = \theta_{n+p} = 1$.

The Hermite QI scheme from [41] provides a spline $Q^{(BS)}_p(g) \in \mathbb{S}_{\boldsymbol{\theta},p}$ which can be written as,

$$Q^{(BS)}_p(g)(\cdot) = \sum_{j=-p}^{n-1} \lambda^{(BS)}_j(g)\ B^{(\boldsymbol{\theta})}_{j,p}(\cdot),$$

where the coefficients $\lambda^{(BS)}_j(g)$, $j = -p, \ldots, n-1$, are defined by the following local linear combinations of g and g' values at the knots,

$$\lambda^{(BS)}_j(g) := \begin{cases} \displaystyle\sum_{i=1}^{p} \hat{\alpha}_i^{(-1,j+p+1)}\, g_{i-1} - \Delta\theta_{k_1} \sum_{i=1}^{p} \hat{\beta}_i^{(-1,j+p+1)}\, g'_{i-1}, \ \ j \le -2, \\ \displaystyle\sum_{i=1}^{p} \hat{\alpha}_i^{(j,p)}\, g_{i+j} - \Delta\theta_{j+k_1+1} \sum_{i=1}^{p} \hat{\beta}_i^{(j,p)}\, g'_{i+j}, \ \ j = -1, \ldots, \hat{n}, \\ \displaystyle\sum_{i=1}^{p} \hat{\alpha}_i^{(\hat{n},j-\hat{n}+p)} g_{\hat{n}+i} - \Delta\theta_{n-k_2} \sum_{i=1}^{p} \hat{\beta}_i^{(\hat{n},j-\hat{n}+p)}\, g_{\hat{n}+i}\,,\ j \ge \hat{n}+1 \end{cases} \tag{31}$$

with $\Delta\theta_j := \theta_j - \theta_{j-1}$, $k_1 := \lfloor p/2 \rfloor$, $k_2 := p - 1 - k_1$, and where for brevity we use the notation $g_s := g(\theta_s)$, $g'_s := g'(\theta_s)$ and $\hat{n} := n - p$. The vectors $\hat{\boldsymbol{\alpha}}^{(j,r)} := (\hat{\alpha}_1^{(j,r)}, \ldots, \hat{\alpha}_p^{(j,r)})^T$ and $\hat{\boldsymbol{\beta}}^{(j,r)} := (\hat{\beta}_1^{(j,r)}, \ldots, \hat{\beta}_p^{(j,r)})^T$ defining the linear combinations in (31) have to be preliminarily computed by solving a suitable local linear system of size $2p \times 2p$. More specifically, $(\hat{\boldsymbol{\alpha}}^{(j,r)T}, \hat{\boldsymbol{\beta}}^{(j,r)T})^T$ is the r-th column of the inverse of a $2p \times 2p$ non singular matrix $G^{(j+k_1+1)}$: the entries of $G^{(j+k_1+1)}$ are the values of all the non vanishing B-splines and their derivatives at the knots $\theta_{j+k_1+1}, \ldots, \theta_{j+k_1+p}$ see [41] for details. For degree $p = 2, 3$ the analytic expression of these coefficient vectors is available; moreover, when a uniform knot distribution is assumed, they do not depend on j, since we are dealing with uniform B-splines. Note that the formulas in (31) can be compactly written in matrix form as follows,

$$(\lambda^{(BS)}_{-p}(g), \ldots, \lambda^{(BS)}_{n-1}(g))^T = \hat{A}^{(p)}\mathbf{g} - \hat{H}\hat{B}^{(p)}\mathbf{g}', \tag{32}$$

where $\hat{H}$ is a diagonal matrix containing the suitable $\Delta\theta$ values and the entries of the matrices $\hat{A}^{(p)}$ and $\hat{B}^{(p)} \in \mathbb{R}^{(n+p)\times(n+p)}$ are defined by using respectively the $\hat{\alpha}$ and $\hat{\beta}$ coefficients in conformity to (31).

We observe that the QI operator $Q^{(BS)}_p$ is a projector in the spline space $\mathbb{S}_{\boldsymbol{\theta},p}$ as proved in [41] and using this fact in it was also seen that the considered QI scheme has maximal approximation order $p+1$ for functions belonging to $C^{p+1}[0\,,\,1]$, provided that the knot distribution is smoothly varying. Note that the last requirement is necessary for the preliminary proof of the existence of an upper bound for the norm of the coefficient vectors $\hat{\boldsymbol{\alpha}}^{(j,r)}$ and $\hat{\boldsymbol{\beta}}^{(j,r)}$ defining the QI. Then, on each element $[\theta_i\,,\,\theta_{i+1}]$ the local approximation error is bounded as:

$$\|g - Q^{(BS)}_p(g)\|_i < \|g - p_i\|_i + \|p_i - Q^{(BS)}_p(g)\|_i,$$

where $\|\cdot\|_i$ means the infinity norm on the considered element, and p_i denotes a local Taylor expansion of degree p of g. Using the preliminary derived upper bound and the projector property of the operator (even if it would be sufficient degree p polynomial reproduction), the well known bound for $\|g - p_i\|_i$ when $g \in C^{p+1}[0\,,\,1]$ allowed to complete the proof. Thus here we can add that, with the same kind of proof, it can be shown also that the approximation order is $\min\{p+1, r+1\}$ when g belongs just to $C^{r+1}[0\,,\,1]$.

The spline $S_g \in \mathbb{S}_{\boldsymbol{\theta},p}$ given by the variant scheme, is instead obtained by approximating the necessary derivative values with symmetric finite difference formulas, i.e. by using the following preliminary approximation,

$$\mathbf{g}' \approx \Gamma^{\ell}\mathbf{g}, \tag{33}$$

where $\mathbf{g} := (g(\theta_0), \ldots, g(\theta_n))^T$ and $\mathbf{g}' := (g'(\theta_0), \ldots, g'(\theta_n))^T$ express the values at the spline knots of g and g' respectively. $\Gamma^{\ell} \in \mathbb{R}^{(n+1)\times(n+1)}$ denotes a $(l+1)$-banded matrix with $\ell_1 = \lfloor l/2 \rfloor$ lower and $\ell - \ell_1$ upper diagonals. The non zero entries of Γ^{ℓ} are such that Eq. (33) gives derivative approximations of order ℓ, where $\ell = p+1$ if p is odd and $\ell = p+2$ otherwise.

Then, considering (32) and (33), S_g can be written as,

$$S_g(\cdot) := \sum_{j=-p}^{n-1} \lambda_j(g)\ B_{j,p}^{(\boldsymbol{\theta})}(\cdot)\,, \quad \text{where} \tag{34}$$

$$(\lambda_{-p}(g)\,, \ldots, \lambda_{n-1}(g))^T := (\hat{C}^{(p)})^T\,\mathbf{g}\,, \text{ with } \hat{C}^{(p)} := (\hat{A}^{(p)} - \hat{H}\,\hat{B}^{(p)}\,\Gamma^{\ell})^T. \tag{35}$$

We observe that, because of the assumed selection of the integer ℓ in (33), S_g keeps the same approximation order of $Q_p^{(BS)}(g)$, although it does not define a projector in $\mathbb{S}_{\boldsymbol{\theta},p}$. Indeed the proposed selection for ℓ guarantees that the error in the derivative approximation has order equal or higher than $p+1$, when $g \in C^{\ell+1}[0\,,\,1]$. As a consequence (32) and (35) imply that for each index the difference $|\lambda_i^{(BS)}(g) - \lambda_i(g)|$ has order at least $p+2$ and so is asymptotically negligible. On the other hand, when $g \in C^{r+1}[0\,,\,1]$ with $r < \ell$, $\Gamma^{\ell}\mathbf{g}$ approximates $\mathbf{g}'$ just with order r. Considering (32) and (35), this implies that for each index the difference $|\lambda_i^{(BS)}(g) - \lambda_i(g)|$ has order $r+1$. Then, using the notation

$$O_A := \min\{p+1, r+1\} \tag{36}$$

and

$$\Delta\theta := \max_{i=1,\ldots,n} \Delta\theta_i\,, \tag{37}$$

the developed analysis can be summarized stating the convergence result reported below in Lemma 1 for the approximation error,

$$e := g - S_g \tag{38}$$

Lemma 1. *Let $g \in C^{r+1}[0\,,\,1]$ and let S_g denote its QI spline approximant of degree p defined in (34) and e the related error defined in (38). Assuming that there exist two positive constants η_1 and η_2 such that,*

$$0 < \eta_1 \leq \frac{\Delta\theta_i}{\Delta\theta_{i+1}} \leq \eta_2\,, i = 1, \ldots, n-1,$$

then there exist positive constants L_j (also depending on $p\,, \eta_1\,, \eta_2$), such that:

$$\|e^{(j)}\|_\infty \leq L_j\,(\Delta\theta)^{O_A - j}\,\|D^{O_A} g\|_\infty\,, \quad j < \min\{p, r+1\}\,, \tag{39}$$

where O_A is defined in (36).

Here we are also interested in analyzing the convergence in the Hölder seminorm, since it will be useful in the next section to obtain convergence results for the developed hypersingular quadrature rules. We recall that $C^{r,\gamma}(0\,,\,1)$, $\gamma \in (0\,,\,1]$, $r \in \mathbb{N}$ is the Hölder space (including $C^{r+1}[0\,,\,1]$) defined as follows,

$$C^{r,\gamma}(0\,,\,1) := \{g \in C^r(0\,,\,1)\,|\,|g^{(r)}|_{0,\gamma} < \infty\},$$

being $|g|_{0,\gamma}$ the seminorm in $C^{0,\gamma}(0\,,\,1)$ defined by

$$|g|_{0,\gamma} := \sup_{x \neq y,\, x,y \in (0\,,\,1)} \frac{|g(x) - g(y)|}{|x-y|^{\gamma}}.$$

In order to prove the following lemma, which is necessary to prove the quadrature convergence order, we first need an intermediate result on pointwise convergence for S_g under the slightly weaker assumption of $g \in C^{r,1}(0\,,\,1)$. We summarize it in the following remark, observing that it can be easily obtained considering the integral form of the rest of the Taylor expansion.

Remark 2. When g belongs to $C^{r,1}(0\,,\,1)$, it can be proved that $|e^{(j)}(x)|$ has order $O_A - j$, $j < \min\{p, r+1\}, \forall x \in (0\,,\,1)$.

Lemma 2. *Let g belong to $C^{r,1}(0\,,1)$, and let S_g denote the p-degree quasi-interpolant of g defined in (34) and e the related error defined in (38). Then there exists a constant $C_p(g)$ depending on g and p (but not on $\Delta\theta$ and j) such that*

$$|e^{(j)}|_{0,\nu} \leq C_p(g)\,(\Delta\theta)^{(O_A - j)(1-\nu)}\,, \quad \forall \nu \in (0\,,\,1)\,,\ \ j < \min\{p\,,\,r+1\}\,, \tag{40}$$

where O_A and $\Delta\theta$ are defined respectively in (36) and in (37).

Proof. Considering that S_g belongs to $C^{p-1}[0\,,\,1]$ and also to $C^{p-1,1}(0\,,\,1)$, taking also into account the smoothness assumptions on g, we can derive that there exists a constant $Q > 1$ such that for each $j < \min\{p\,,\,r+1\}$, $\forall x, y \in (0\,,\,1)$, it is

$$|e^{(j)}(x) - e^{(j)}(y)| \leq |g^{(j)}(x) - g^{(j)}(y)| + |S_g^{(j)}(x) - S_g^{(j)}(y)| \leq Q|x-y|.$$

Since we can write

$$\frac{|e^{(j)}(x) - e^{(j)}(y)|}{|x-y|^\nu} = |e^{(j)}(x) - e^{(j)}(y)|^{1-\nu} \left(\frac{|e^{(j)}(x) - e^{(j)}(y)|}{|x-y|}\right)^\nu,$$

from the previous inequality it also follows that

$$\frac{|e^{(j)}(x) - e^{(j)}(y)|}{|x-y|^\nu} \leq Q^\nu |e^{(j)}(x) - e^{(j)}(y)|^{1-\nu} \leq Q|e^{(j)}(x) - e^{(j)}(y)|^{1-\nu}.$$

As x and y are arbitrary values in $(0,\,1)$, taking into account Remark 2, we can conclude the proof. □

5. Quadrature rules for hypersingular integrals

In this section we are interested in using the quasi-interpolation scheme previously introduced to approximate the hypersingular integral defined in (26), where w is a non negative weight function. Concerning the smoothness requirements, we make the standard assumption that both w and g belong at least to $C^{m,\gamma}(0\,,\,1), \gamma \in (0\,,\,1]$, see [53,54] for an introduction and more details.

The proposed rule approximates $I_{w,m}[g,\sigma]$ with the following integral which can be exactly computed,

$$I_{w,m}^{Q,p}[g,\sigma] := \fint_0^1 w(\tau)\frac{S_g(\tau)}{(\tau-\sigma)^{m+1}}\,d\tau\,,$$

where S_g is the $C^{p-1}[0\,,\,1]$ spline of degree $p \geq m+1$ defined in (34) which quasi-interpolates g. In particular, having in mind the applications to IgA-SGBEMs where $m = 1$, we will focus on the cases $w \equiv 1$ and $w = B$, that is a B-spline function of degree $d \geq 2$ with support equal to $[0\,,\,1]$ and which belongs at least to $C^1[0\,,\,1]$. For $w \equiv 1$, considering (34), we have that

$$I_{1,m}^{Q,p}[g,\sigma] = \mathbf{w}(\sigma)^T\mathbf{g}\,,$$

where $\mathbf{g} := (g(\theta_0),\ldots,g(\theta_n))^T$ is the vector collecting the values of the function g at the quadrature nodes, while the weight vector $\mathbf{w}(\sigma)$ is defined as,

$$\mathbf{w}(\sigma) := \hat{C}^{(p)}\boldsymbol{\mu}^{(p)}(\sigma),$$

with $\hat{C}^{(p)}$ being the matrix used to define S_g (see formula (35)), and $\boldsymbol{\mu}^{(p)}(\sigma) := (\mu_{-p}^{(p)},\ldots,\mu_{n-1}^{(p)})^T$ denoting the vector of the *modified moments* given by

$$\mu_j^{(p)} = \mu_j^{(p)}(\sigma) := \fint_0^1 B_{j,p}^{(\boldsymbol{\theta})}(\tau)\,\frac{1}{(\tau-\sigma)^{m+1}}\,d\tau\,, \quad j = -p,\ldots,n-1. \tag{41}$$

When $w \equiv B$, we preliminarily use the spline product algorithm proposed in [38] to express in B-spline form the product $B\ S_g$ which is a spline of degree $d+p$ in $[0\,,\,1]$. Such spline belongs to a product space Π of dimension P with knots and related multiplicities suitably obtainable from those of B and S_g. With this preliminary step we obtain

$$I_{B,m}^{Q,p}[g,\sigma] = \mathbf{w}^{(B)}(\sigma)^T\mathbf{g}\,,$$

where this case

$$\mathbf{w}^{(B)}(\sigma) := \hat{C}^{(p)}\ G^{(p,d)}\ \boldsymbol{\mu}^{(p+d)}(\sigma),$$

with $G^{(p,d)} \in \mathbb{R}^{(n+p)\times P}$ denoting the matrix collecting the B-spline coefficients of the product $B\ S_g$ (see [38] for details), and $\boldsymbol{\mu}^{(p+d)}(\sigma) \in \mathbb{R}^P$ is the vector of the modified moments associated with the B-spline basis of Π.

5.1. Modified moments computation

The *modified moments* defined in Eq. (41) can be exactly computed by the recursive approach introduced in [26, Section 3.2]. For the sake of completeness here we briefly summarize their derivation. By setting,

$$I_q(B^{(\boldsymbol{\theta})}_{j,r}, \sigma) := \neq\!\!\!\!\int_0^1 B^{(\boldsymbol{\theta})}_{j,r}(\tau)\, \frac{\tau^q}{(\tau-\sigma)^{m+1}}\, d\tau\,, \qquad q \in \mathbb{N},$$

we have that in particular,

$$\mu^{(p)}_j = I_0(B^{(\boldsymbol{\theta})}_{j,p}, \sigma).$$

Taking into account the recurrence relation of B-splines:

$$B^{(\boldsymbol{\theta})}_{j,r}(\tau) \;=\; \omega_{j,r}(\tau)\, B^{(\boldsymbol{\theta})}_{j,r-1}(\tau) \;+\; (1-\omega_{j+1,r}(\tau))\, B^{(\boldsymbol{\theta})}_{j+1,r-1}(\tau)\,,$$

with

$$\omega_{j,r}(\tau) := \begin{cases} \frac{\tau-\tau_j}{\tau_{j+r}-\tau_j} & \text{if } \tau_j < \tau_{j+r}\,, \\ 0 & \text{otherwise} \end{cases},$$

we can obtain a recurrence formula for the integrals $I_q(B^{(\boldsymbol{\theta})}_{j,r}, \sigma)$:

$$\begin{aligned} I_q(B^{(\boldsymbol{\theta})}_{j,r}) \;&=\; \left(I_{q+1}(B^{(\boldsymbol{\theta})}_{j,r-1}) - \tau_j\, I_q(B^{(\boldsymbol{\theta})}_{j,r-1})\right)/(\tau_{j+r}-\tau_j) + \\ &\quad \left(\tau_{j+r+1}\, I_q(B^{(\boldsymbol{\theta})}_{j+1,r-1}) - I_{q+1}(B^{(\boldsymbol{\theta})}_{j+1,r-1})\right)/(\tau_{j+r+1}-\tau_{j+1})\,, \end{aligned} \tag{42}$$

where for brevity we have omitted the dependency on the σ parameter. We remark that, when multiple knots are taken, if $\tau_{j+r} = \tau_j$ ($\tau_{j+r+1} = \tau_{j+1}$), the first (second) addend on the right-hand side of (42) must be set to zero. Then the computation of the $\mu^{(p)}_j = I_0(B^{(\boldsymbol{\theta})}_{j,p})$ requires the preliminary computation of $I_k(B^{(\boldsymbol{\theta})}_{i,0})$, for $k = 0, \ldots, p$ and $i = -p, \ldots, n-1$. Now, considering that

$$B^{(\boldsymbol{\theta})}_{i,0}(\tau) = \begin{cases} 1 & \text{if } \tau_i \le \tau < \tau_{i+1}\,, \\ 0 & \text{otherwise}\,, \end{cases}$$

we obtain that $I_k(B^{(\boldsymbol{\theta})}_{i,0}) = \int_{\tau_i}^{\tau_{i+1}} B^{(\boldsymbol{\theta})}_{i,0}(\tau)\, \frac{\tau^k}{(\tau-\sigma)^{m+1}}\, d\tau$, which clearly is a vanishing quantity if $\tau_i = \tau_{i+1}$. In the opposite case, using the substitution $z = \tau - \sigma$ we can write,

$$I_k(B^{(\boldsymbol{\theta})}_{i,0}) = \sum_{j=0}^{k} \binom{k}{j} \sigma^{k-j} \int_{\tau_i-\sigma}^{\tau_{i+1}-\sigma} z^{j-m-1}\, dz\,.$$

We observe that the above relation involves integrals of powers also with negative exponent ranging from -1 to $-m-1$ which are singular if $\sigma \in [\tau_i, \tau_{i+1}]$. In such cases they have to be interpreted as Cauchy principal values for $j = m$ and $\sigma \in (\tau_i, \tau_{i+1})$ and as HFP otherwise.

Remark 3. From the computational point of view the method we propose reveals a remarkable saving in terms of function evaluations. Indeed, the quadrature scheme is designed on the whole support of the B-spline trial functions rather than element-by-element as in the classical approach. The hypersingular kernel needs no regularization and it is never evaluated, being incorporated in the computation of the modified moments which is done following the recurrence relations described in Section 5.1. On the other hand, some computational effort is needed in order to get the necessary accuracy to keep the overall good approximation properties, as pointed out in [28] and [55]. Nevertheless, the involved quantities can be pre-computed and stored at least when uniform spacing is adopted, as all the shape functions are obtained by shifting one instance, see [55, Section 3.2]. Therefore the overall cost is reduced and in all tested cases never becomes prohibitive.

5.2. Convergence of QI hypersingular integration formulas

In this subsection we derive two convergence results for the quadrature rule $I^{Q,p}_{w,m}[g,s]$, presenting them in the following two theorems. Theorem 1 concerns the general case of $g \in C^{r,1}(0,1)$, generically assuming $\sigma \in (0,1)$, and it is proved extending to quasi-interpolating splines the arguments used in [56] for spline interpolants. On the other hand Theorem 2 concerns the special case of $p \geq r$ and σ admitting a neighborhood $\mathcal{I}_\sigma$ such that $g \in C^{r,1}(0,1) \cap C^{p,1}(\mathcal{I}_\sigma)$. Such new theorem is of interest to fully explain the experimental results reported in the next subsection. In both theorems we use the following notation to denote the hypersingular quadrature error,

$$R_{\Delta\theta,m,p}[g,\sigma] := I_{w,m}[g,\sigma] - I^{Q,p}_{w,m}[g,\sigma] = I_{w,m}[g,\sigma] - I_{w,m}[S_g,\sigma]. \tag{43}$$

We observe that in [27] it was proved that, when applied to weakly singular or even singular integrals, the considered quadrature rules have a superconvergence behavior when p is even and the quadrature nodes are uniform. Unfortunately, this feature is lost in the hypersingular case, as shown in the first experiment reported in the following subsection (see Fig. 1). Indeed in this section we will prove that under suitable smoothness requirements the pth rule has always convergence order p which is the standard in the hypersingular case.

Theorem 1. *Let $w \in C^{m,\gamma}(0,1), \gamma \in (0,1], m \in \mathbb{N}^+$, be a nonnegative weight and let g belong to $C^{r,1}(0,1), r \geq m$ and $\sigma \in (0,1)$. If $p \geq m+1$, then the quadrature error defined in (43) is in general of order $O\left((\Delta\theta)^{(O_A-m)(1-\nu)}\right)$, $\forall \nu \in (0,1)$, where O_A and $\Delta\theta$ are defined respectively in (36) and in (37).*

Proof. Clearly it holds

$$R_{\Delta\theta,m,p}[g,s] = \fint_0^1 w(\tau)\frac{e(\tau)}{(\tau-\sigma)^{m+1}}\,d\tau,$$

where $e = g - S_g$ is the approximation error. Now, being $r \geq m$, we have that $g \in C^{m,1}(0,1)$. Similarly, being $p \geq m+1$, it descends that $S_g \in C^{m,1}(0,1)$. Thus, $e \in C^{m,\nu}(0,1), \forall \nu \in (0,1)$, being $C^{m,1}(0,1) \subset C^{m,\nu}(0,1)$. Using the Taylor expansion of e of degree $m-1$ at $\tau = \sigma$ and the corresponding error expression in Lagrange form, we have,

$$R_{\Delta\theta,m,p}[g,\sigma] = \sum_{j=0}^{m-1}\frac{e^{(j)}(\sigma)}{j!}\fint_0^1 w(\tau)\frac{1}{(\tau-\sigma)^{m+1-j}}\,dt + \int_0^1 w(\tau)\frac{e^{(m)}(\xi_{\tau,\sigma})}{m!\,(\tau-\sigma)}\,d\tau,$$

where $\xi_{\tau,\sigma}$ is a point between σ and τ. The second addend on the right-hand side can also be written as,

$$\frac{1}{m!}\int_0^1 \frac{w(\tau)}{(\tau-\sigma)^{1-\nu}}\frac{e^{(m)}(\xi_{\tau,\sigma}) - e^{(m)}(\sigma)}{(\tau-\sigma)^{\nu}}\,d\tau + \frac{1}{m!}e^{(m)}(\sigma)\fint_0^1 \frac{w(\tau)}{(\tau-\sigma)}\,d\tau.$$

Thus we obtain,

$$|R_{\Delta\theta,m,p}[g,\sigma]| \leq \sum_{j=0}^{m-1}\frac{|e^{(j)}(\sigma)|}{j!}\,|\mathcal{I}_{j,\sigma,m}| + |e^{(m)}|_{0,\nu}\frac{1}{m!}\mathcal{J}_{\sigma,\nu} + |e^{(m)}(\sigma)|\frac{1}{m!}|\mathcal{Q}_\sigma|$$

with

$$\mathcal{I}_{j,\sigma,m} := \fint_0^1 w(\tau)\frac{1}{(\tau-\sigma)^{m+1-j}}\,d\tau,\quad \mathcal{J}_{\sigma,\nu} := \int_0^1 \frac{w(\tau)}{|\tau-\sigma|^{1-\nu}}\,d\tau,$$
$$\mathcal{Q}_\sigma := \int_0^1 \frac{w(\tau)}{(\tau-\sigma)}\,d\tau.$$

Since the integrals defining $\mathcal{I}_{j,\sigma,m}$, $\mathcal{J}_{\sigma,\nu}$ and $\mathcal{Q}_\sigma$ are all finite because of the assumptions on w, considering (40) the proof is concluded. □

Theorem 2. *Let $w \in C^{m,\gamma}(0,1), \gamma \in (0,1], m \in \mathbb{N}^+$, be a nonnegative weight and let g belong to $C^{r,1}(0,1), r \geq m$. If $p \geq r$ and there exists a neighborhood $I_\sigma \subset (0,1)$ of $\sigma \in (0,1)$ such that $g \in C^{p,1}(I_\sigma)$, then the quadrature error defined in (43) is in general of order $O\left((\Delta\theta)^{\min\{(p+1-m)(1-\nu),r+1\}}\right)$, $\forall \nu \in (0,1)$, where $\Delta\theta$ is defined in (37).*

Proof. Consider first of all that, if $\hat{I}_\sigma$ is a neighborhood of σ strictly included in I_σ, there exists $\hat{h}$ such that, if $\Delta\theta \leq \hat{h}$, the same result proved in Remark 2 can be proved in $\hat{I}_\sigma$, where locally $O_A = p+1$, thanks to the regularity assumption on g in I_σ. Now we can split $R_{\Delta\theta,m,p}[g,\sigma]$ into $R_N + R_E$, where $R_N := R_{\Delta\theta,m,p}[g|\hat{I}_\sigma,\sigma]$ and R_E is the remaining part of the integral which is not anymore singular. Concerning R_N, we observe that preliminarily Lemma 2 and then Theorem 1 can be locally proved in $\hat{I}_\sigma$, setting in this case $O_A = p+1$. Concerning R_E, since the approximation error $e = g - S_g$ has just order $r+1$ when $x \in (0,1) \setminus \hat{I}_\sigma$, considering that the integral defining R_E is not anymore singular, we can anyway conclude that R_E belongs to $O(\Delta\theta^{r+1})$. Thus the thesis follows. □

5.3. Numerical experiments on hypersingular quadrature

In this section we present some experimental results on the adopted hypersingular quadrature rules which have been tested for the integral in (26) with $m = 1$ and both the choices $w \equiv 1$ and $w = B$, with B denoting in particular the quadratic uniform B-spline with support in [0, 1] and simple knots. These experiments are aimed to verify that for both the considered weights we can do the same analysis and also to test the performances of the adopted rules under different smoothness properties of the function g. Note that, in order to have a reference value to define suitably $I_{w,1}[g,\sigma]$ which is necessary for the error computation, for these experiments we have always precomputed the value produced by the same quadrature rule applied with 2000 uniform nodes. In particular in the figures the behavior for increasing n of the following maximum quadrature error Err_M is always shown,

$$Err_M := \max_{\sigma\in\mathcal{R}} |I_{w,1}[g,\sigma] - I^{Q,p}_{w,1}[g,\sigma]|\,, \tag{44}$$

where $\mathcal{R}$ denotes the considered set of values where σ ranges.

In Fig. 1 we take $g(\tau) = e^\tau$ and for both the considered weight functions we set $\mathcal{R} = \{0, 0.1, \ldots, 0.9, 1\}$. Looking at the figure, we can verify that, varying the QI degree p, the theoretical optimal order is always observed, according to Theorem 1. Note also that, as expected, the reduced regularity of the second weight does not affect the accuracy of the quadrature rules.

Referring to this experiment and focusing on accuracy/number of quadrature nodes, we have also compared our rules with those based on gaussian quadrature and on kernel regularization which were introduced in [47]. The aim of such a comparison is to show that the last ones are not suited for our current IgA-BEM code which adopts a function-by-function assembly strategy. Note that for these additional tests we had to exclude $\sigma = 0$ and $\sigma = 1$ from the experiments, since the rules proposed in [47] cannot be applied when the singularity is at the extremes of the integration domain. For the case $w \equiv 1$, actually the formulas in [47] are very effective, since an accuracy already of order 10^{-7} is obtained just by using 7 quadrature nodes. Conversely, as shown in Table 1, when w is a B-spline the results deteriorate (to obtain accuracy of order 10^{-3} for all $\sigma \in \mathcal{R} \setminus \{0, 1\}$, at least 112 gaussian nodes are necessary). On this concern we comment that the better behavior for $w = 1$ of the alternative rules was expected, since for smooth functions gaussian formulas are probably the best choice, being characterized by maximal polynomial exactness. Since for IgA-SGBEM and also general IgA-BEM applications the B-spline weight is included in the integrand and also the factor g is not highly smooth, their superiority in the smooth case is not very significant in such context.

Fig. 2 considers for the same weights a less regular function. In this case $g(\tau) = S_2$, with S_2 denoting the spline of degree six and uniform breakpoints in $\mathcal{S} = \{0, 0.25, 0.5, 0.75, 1\}$ with just C^2 smoothness at such points, belonging anyway to $C^{2,1}(0, 1)$. In particular the plots shown in Figs. 2(a) and 2(b) relate to the case $\mathcal{R} \cap \mathcal{S} = \emptyset$, since we fix $\mathcal{R} = \{0.2, 0.4, 0.6, 0.8\}$, while those in Fig. 2(c) and 2(d) to the case $\mathcal{R} = \mathcal{S}$. Looking at the pictures on the upper part of the figure we can first of all observe that, when $\mathcal{R} \cap \mathcal{S} = \emptyset$, the convergence order is not so clear, resulting for $p = 4$ even better than expected from Theorem 2. On the other hand, the lower part of the figure clearly shows that when $\mathcal{R} = \mathcal{S}$, the convergence order of the rules deteriorates becoming equal to 2 for any p, as expected from Theorem 1. The rules have been tested also for $g(\tau) = S_1$, with S_1 denoting the spline of degree six with breakpoints in $\mathcal{S}$ and with just C^1 smoothness at such points. Since the achieved results are qualitatively analogous to those obtained for S_2, for brevity we omit them (the convergence order of the rules again significantly deteriorates only for $\mathcal{R} = \mathcal{S}$, becoming in such case equal to 1).

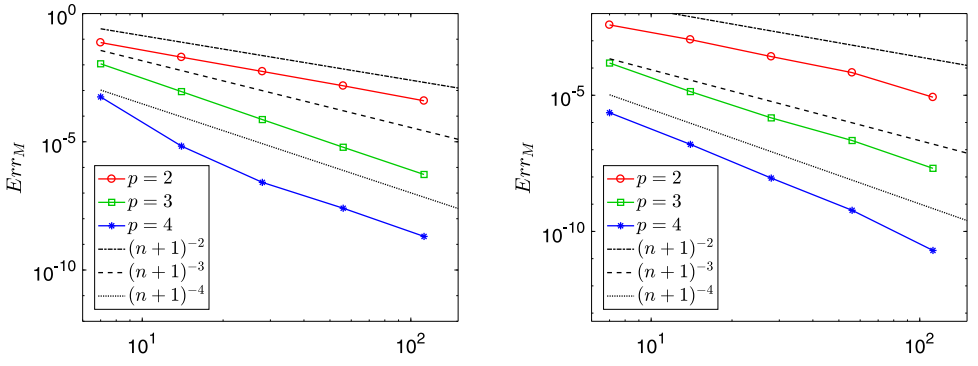

(a) $w \equiv 1$ (b) $w = B$ (C^1 quadratic B-spline)

Fig. 1. Convergence behavior of the maximum quadrature error Err_M defined in (44) for the function $g = \exp$..

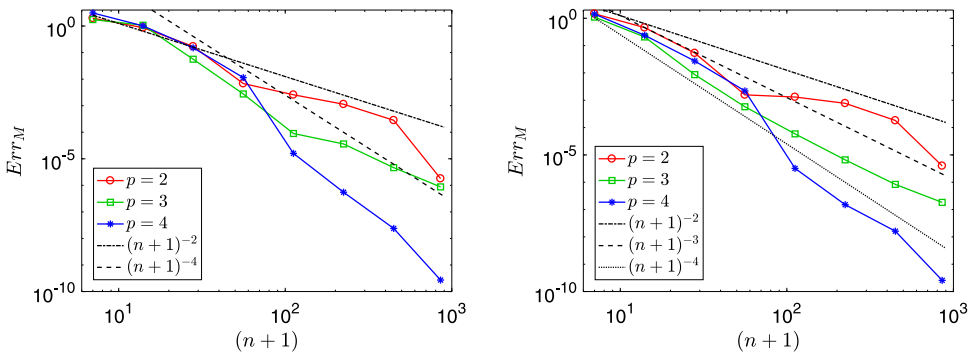

(a) $\mathcal{R} \cap \mathcal{S} = \emptyset$, $w \equiv 1$. (b) $\mathcal{R} \cap \mathcal{S} = \emptyset$, $w = C^1$ quadratic B-spline

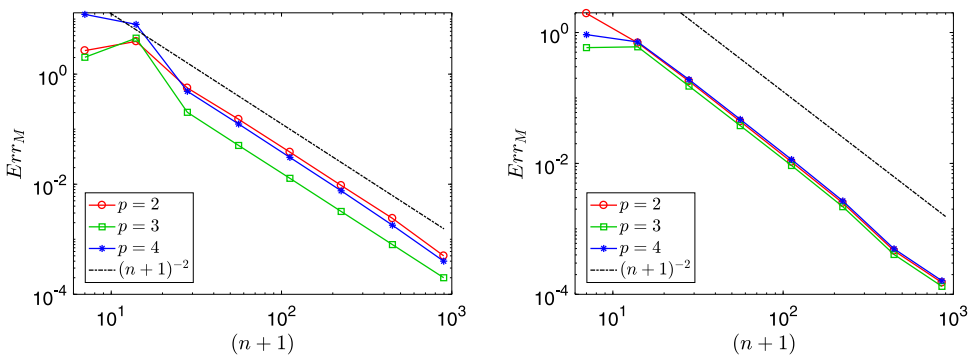

(c) $\mathcal{R} = \mathcal{S}$, $w \equiv 1$. (d) $\mathcal{R} = \mathcal{S}$, $w = C^1$ quadratic B-spline

Fig. 2. Convergence behavior of the maximum quadrature error Err_M defined in (44) for $g = S_2$, a C^2 sestic spline.

Table 1
Convergence behavior of the maximum quadrature error (maximum error for $\sigma \in \mathcal{R} \setminus \{0\,,\ 1\}$) characterizing the rules introduced in [47] for the function $g = \exp$ and $w = B$.

$n+1$	7	14	28	56	112
Error	$9.2 \cdot 10^{-1}$	$8.2 \cdot 10^{-2}$	$4.8 \cdot 10^{-2}$	$9.3 \cdot 10^{-3}$	$1.1 \cdot 10^{-3}$

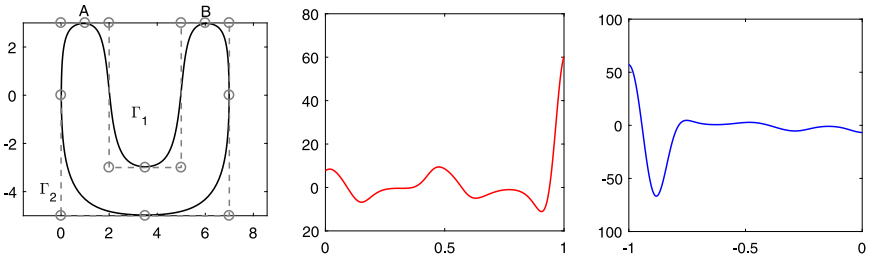

(a) Geometry. (b) Exact flux q on Γ_1. (c) Exact potential u on Γ_2.

Fig. 3. Example 1: U shape domain.

6. Applications to IgA-SGBEM

In this section four 2D Laplace problems are considered, two with mixed and two with pure Neumann boundary conditions. In the experiments the weights used to define the boundaries as in (11)–(12) are all always unit values, except for Example 3 where suited weights are used to obtain an exact parametric representation of the considered elliptical boundary [57]. In every experiment all the breakpoints of the splines defining the test spaces $V_h^{(i)}$, $i = 1, 2$ are uniformly spaced and they are (a refinement of) the breakpoints used to define $\mathbb{S}$. Uniform spacing is adopted also for the quadrature nodes. The final convergence order of $u_h - u$ (and $q_h - q$ for mixed problems) is reported. The accuracy of the quadrature rules when $g = g_\sigma^{(k)}$, i.e., g is the function defined in (27), for all $k = 1, \ldots, N_2$ is also studied. Thus the behavior of the following quantity for n increasing is shown,

$$Err_{MM} := \max_{k=1,\ldots,N_2} \{ \max_{\sigma \in \mathcal{R}_k} |I_{w,1}[g_\sigma^{(k)}, \sigma] - I_{w,1}^{Q,p}[g_\sigma^{(k)}, \sigma]| \}, \tag{45}$$

where $\mathcal{R}_k$ is obtained as the image through the linear mapping $\mathcal{L}_k$ of a given set $\mathcal{R}$ of abscissas in $[a_2\,,\, b_2]$.

Example 1: U shape geometry

In the first example we consider a U-shaped geometry globally described by a B-spline curve $\mathbf{F}$ of degree 4, hence $d_1 = d_2 = 4$, and maximal regularity C^3 defined on the parametric interval $[-1, 1]$ and with a uniform extended knot vector $T = 1/7(-11, -10, \ldots, 10, 11)$. The sections of the boundary corresponding to Γ_1 and Γ_2 are considered between the points $A = \mathbf{F}(0)$ and $B = \mathbf{F}(-1) = \mathbf{F}(1)$, as it is shown in Fig. 3(a) where the control points are also shown. For more clarity, referring to the notation introduced in formula (11) and reported in Section 3, we precise that here $\mathbf{F}_1 = \mathbf{F}|_{[0\,,\,1]}$ and $\mathbf{F}_2 = \mathbf{F}|_{[-1\,,\,0]}$. A mixed boundary value problem (1) is assayed with,

$$u^*(x_1, x_2) := \sin x_1 \cosh x_2\,,\ (x_1, x_2) \in \Gamma_1\,, \quad q^*(x_1, x_2) := \frac{\partial u^*}{\partial \mathbf{n}},\ (x_1, x_2) \in \Gamma_2.$$

The exact solution is also depicted in Fig. 3: the exact flux q in 3(b) and the exact potential u in 3(c).

According to the IgA paradigm, quartic B-splines are employed for the approximation of u, while cubics are used for q, since it exhibits a reduced regularity: q in this example is C^2 smooth, involving the first derivative of the geometry mapping $\mathbf{F}_1$. For the quadrature in this test we employ degree $p = 4$ and a number of uniform nodes $n+1$ in (26) equal to 11, which means that the quadrature nodes are the knots of the weight B and their midpoints. Note that in this case, for every value of σ, the integrand function $g_\sigma^{(k)}$ in (27) is globally at least C^2 smooth for each k and each σ. Fig. 4 shows the convergence behavior of the quadrature error Err_{MM} defined in (45). In particular in Fig. 4(a) we assume $\mathcal{R} = \{-0.8, -0.7, \ldots, -0.1\}$ which implies that $\mathcal{R} \cap T = \emptyset$, while in Fig. 4(b) $\mathcal{R}$ is the set of breakpoints defining $\mathbf{F}_2$. The figure clearly shows that there is a reduction of the convergence order to 2 only in the second case.

Concerning the final results produced by our current IgA-SGBEM implementation, Fig. 5 shows that, with respect to both the L^∞ and L^2 norm, the approximation error $u_h - u$ has convergence order $O(h^5)$ while the flux error $q_h - q$ has order $O(h^4)$.

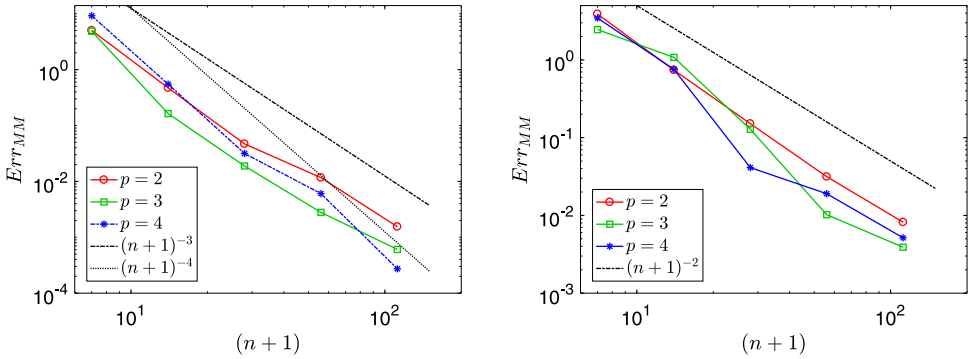

(a) $\mathcal{R} \cap T = \emptyset$. (b) $\mathcal{R} \subset T_2$.

Fig. 4. Example 1: convergence behavior of the maximum quadrature error Err_{MM}.

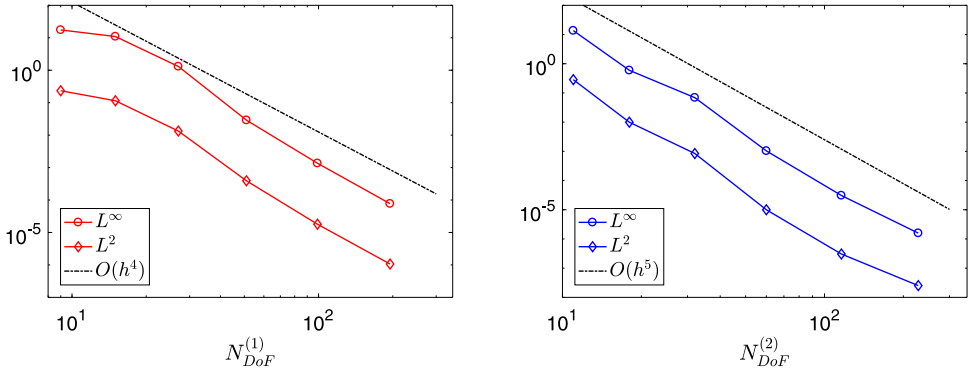

(a) Approximation error $q_h - q$. (b) Approximation error $u_h - u$.

Fig. 5. Example 1: U shape domain. Approximation errors in both the L^∞ and L^2 norms.

Example 2: domain with a hole

In this example we consider another mixed boundary value problem (1), where

$$u^*(x_1, x_2) := e^{x_1} \sin x_2\,, \ (x_1, x_2) \in \Gamma_1\,, \quad q^*(x_1, x_2) := \frac{\partial u^*}{\partial \mathbf{n}}, \ (x_1, x_2) \in \Gamma_2.$$

The problem is formulated on the doubly connected domain shown in Fig. 6(a). Fig. 6 shows also the exact solution which is again a priori known, the exact flux q in Fig. 6(b) and exact potential u in Fig. 6(c). Each curve Γ_i defining the boundary is parameterized by a cubic B-spline $\mathbf{F}_i\,, i = 1, 2$, hence $d_1 = d_2 = 3$, with maximal regularity C^2. The parameterization $\mathbf{F}_1$ is defined in $[-1\,,\ 1]$ with respect to $T_1 = 1/4(-7, -6, \ldots, 6, 7)$, while $\mathbf{F}_2$ is defined in $[4\,,\ 6]$ with respect to the extended uniform knot vector $T_2 = 1/4(13, 14, \ldots, 26, 27)$. The control points are shown in Fig. 6(a).

Since the assumption in (14) is always adopted, for this experiment cubic and quadratic splines are used to approximate u and q, respectively. Furthermore, we set $p = 3$ and $n + 1 = 13$, i.e. the quadrature nodes are the knots of the weight B and two additional interior equidistant nodes per element. Note that in this case $g_\sigma^{(k)}$ in (27) is just globally C^1 smooth, but it remains C^2 at $\tau = \sigma$: it is globally smoother only if further h refinement has already been applied and the support of B_{k,d_2} does not include any original breakpoint of $\mathbf{F}_2$. Indeed, the function ρ defined in (28) can be continuously extended to a function continuous in $[a_2\,,\ b_2]$. Fig. 7 confirms that the quadrature error deteriorates only for $\mathcal{R} \subset T_2$ and again the convergence order in this case becomes equal to the regularity of $g_\sigma^{(k)}$ at $\tau = \sigma$.

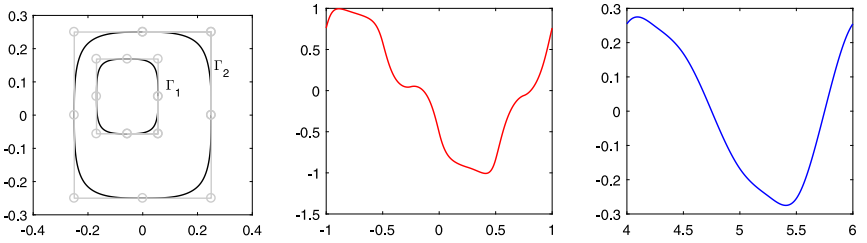

(a) Geometry. (b) Exact flux q on Γ_1. (c) Exact potential u on Γ_2.

Fig. 6. Example 2: domain with a hole.

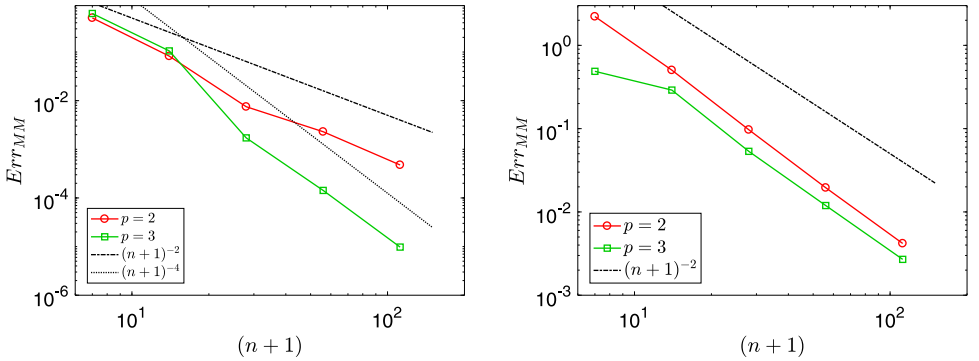

(a) $\mathcal{R} \cap T_2 = \emptyset$. (b) $\mathcal{R} \subset T_2$.

Fig. 7. Example 2: convergence behavior of the maximum quadrature error Err_{MM}.

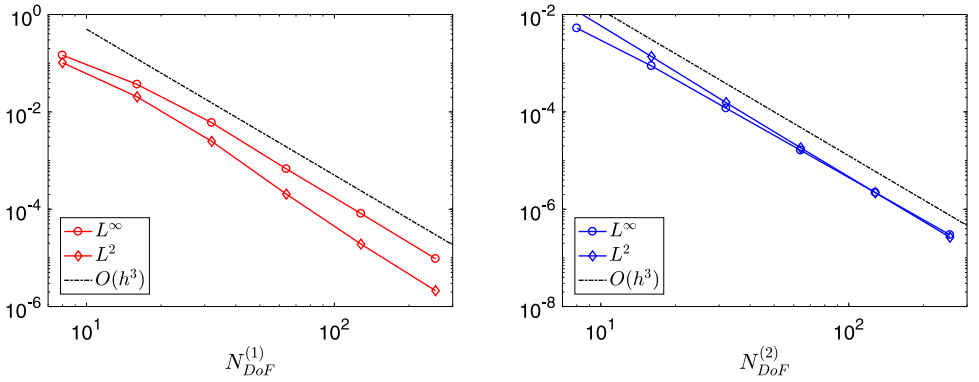

(a) Approximation error $q_h - q$. (b) Approximation error $u_h - u$.

Fig. 8. Example 2: domain with a hole. Approximation errors in both the L^∞ and L^2 norms.

Figs. 8(a) and 8(b) report the L^∞ and the L^2 norms of the final errors, showing that convergence rate $O(h^3)$ is obtained for both $u_h - u$ and $q_h - q$.

Example 3: interior Neumann

For the third example we consider the pure Neumann problem analyzed in [47], interior to an ellipse centered at the origin and with semi axes of length 2 and 4. The boundary of the elliptical domain is represented using quadratic

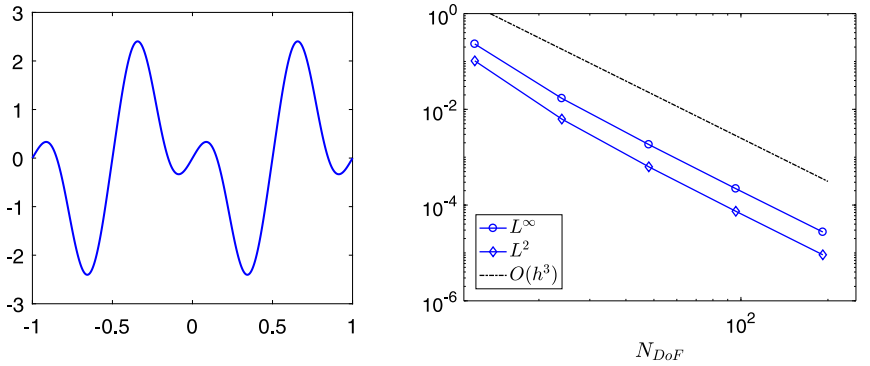

(a) Exact solution u_0. (b) $\|u_h - u\|$ in both the L^∞ and L^2 norms.

Fig. 9. Example 3: Neumann problem interior to an ellipse.

NURBS with double inner knots defined in the parameter domain $[-1\,,\,1]$, with uniform breakpoints determining four rational arcs. Note however that, thanks to symmetries in the control polygon, $\mathbf{F} = \mathbf{F}_2$ is C^1 smooth for this test. The exact solution reads $u = u_c := x_1^3 x_2 - x_1 x_2^3 + c$, with $c \in \mathbb{R}$. In particular we search for the solution having vanishing integral on the boundary, i.e., u_0, see Fig. 9(a).

For the quadrature we set $p = 2$ and $n + 1 = 13$. Again our experiments confirm the convergence behavior previously observed for the quadrature rules. Note that also in this case the function ρ defined in (28) can be continuously extended to a function continuous in $[a_2\,,\,b_2]$.

The behavior of $u_h - u$ in both the L^∞ and L^2 norms is reported in Fig. 9(b). The optimal convergence rate $O(h^3)$ is steadily observed, see [46].

Example 4: screen problem

The last considered example is the Neumann problem defined in (7), with $\partial\Omega = \{\mathbf{x} = (x, y) \in \mathbb{R}^2 | \, 0 \leq x \leq 1, y = 0\}$. This is also called a screen problem and the unknown ϕ, vanishing at the endpoints of $\partial\Omega$, represents the jump of u across the obstacle. For the given datum $q^* = 1$, the analytical solution is known and it reads: $\phi(\mathbf{x}) = 2\sqrt{x(1-x)}$. The boundary is represented in terms of quadratic B-splines ($d_2 = 2$) defining a C^∞ function $\mathbf{F} = \mathbf{F}_2$. For the quadrature $p = 2$ and $n + 1 = 7$ are chosen. This is a peculiar example for which global refinement would not output the optimal convergence rate, as the solution exhibits a reduced regularity at the end points. Therefore, we consider the error estimates given in [58, Theorem 2.2] which states that in the L^2 norm the expected optimal order of convergence is $O(h^{1-2\varepsilon})$, while in the energy norm it is $O(h^{1/2-\varepsilon})$ for any $\varepsilon > 0$. The error in the energy norm is obtained as $\sqrt{|||\phi|||^2 - |||\phi_h|||^2}$, with $|||\phi|||^2 = \langle D\phi, \phi\rangle_{L^2(\partial\Omega)} = \pi/4$ and $|||\phi_h|||^2 = \langle D\phi_h, \phi_h\rangle_{L^2(\partial\Omega)} = \boldsymbol{\alpha}^\top A\boldsymbol{\alpha}$, with A denoting the Galerkin matrix and $\boldsymbol{\alpha}$ the vector of coefficients, as in (15).

Fig. 10 shows that the obtained results confirm the theoretical estimates. Note that, adopting the alternative quadrature rules introduced in [47] and already mentioned for comparison purposes in the first test case considered in Sub Section 5.3, the same convergence behavior can be obtained in both the considered norms if at least 8 gaussian nodes for element, that is 24 for each B-spline support, are used.

7. Conclusions

Quadrature rules based on spline quasi-interpolation (QI) are introduced for the numerical approximation of hypersingular integrals, also including a B-spline weight. Under suitable smoothness requirements for the integrand factor g approximated by the QI scheme, it is first proved that the proposed rules exhibit optimal convergence order. Then their convergence behavior is investigated assuming reduced smoothness of g. Finally, the application of the rules within the IgA-SGBEM method for the numerical solution of 2D Laplace problems, with mixed or pure Neumann boundary conditions, is studied. In all the considered IgA-SGBEM experiments the expected convergence

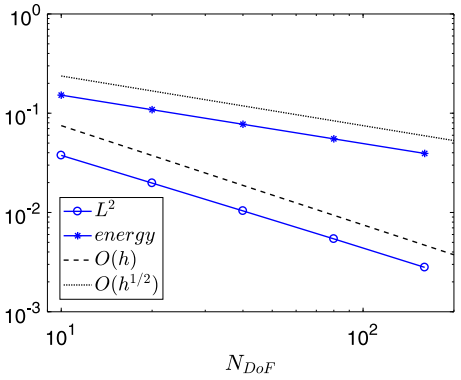

Fig. 10. Example 4: screen problem. Approximation error $u_h - u$ versus N_{DOF} in both the L^2 and energy norms.

order of the discretization scheme is guaranteed by using very few uniform quadrature nodes in the support of each B-spline test function.

These results conclude the study of the 2D case and have been considered as the basis for the analysis of the 3D case. We observe however that the extension to the 3D case is not straightforward, even if tensor-product topology, to some extent, allows us to exploit the techniques developed in the 2D case. New aspects and challenges in particular have to be considered for the treatment of kernel singularities, since in 3D a singular kernel fully independent of the geometry parameterization cannot be derived and also because advanced strategies for the kernel splitting are necessary to guarantee sufficient smoothness to the functions approximated by the QI operator used in our rules: some preliminary results are available in [59].

Declaration of competing interest

The authors declare that they have no known competing financial interests or personal relationships that could have appeared to influence the work reported in this paper.

Acknowledgments

The authors are members of the INdAM Research group GNCS. The INdAM support through GNCS “Progetti di Ricerca 2018–2020” programs and Finanziamenti Premiali SUNRISE is gratefully acknowledged. A. Falini was also supported by the INdAM-GNCS project “Finanziamenti Giovani Ricercatori 2019–2020”.

References

[1] G. Chen, J. Zhou, Boundary Element Methods, second ed., World Scientific Publishing Co., Inc. River Edge, NJ, USA, 2010, p. 700.
[2] A. Aimi, M. Diligenti, C. Guardasoni, Energetic BEM for the numerical analysis of 2D Dirichlet damped wave propagation exterior problems, Commun. Appl. Ind. Math. 9 (1) (2017) 1–25.
[3] A. Aimi, C. Guardasoni, Collocation boundary element method for the pricing of geometric Asian options, Eng. Anal. Bound. Elem. 92 (2018) 90–100.
[4] S. Bertoluzza, S. Falletta, FEM solution of exterior elliptic problems with weakly enforced integral non reflecting boundary conditions, J. Sci. Comput. 81 (2) (2019) 1019–1049.
[5] L. Heltai, J. Kiendl, A. DeSimone, A. Reali, A natural framework for isogeometric fluid–structure interaction based on BEM–shell coupling, Comput. Methods Appl. Mech. Engrg. 316 (2017) 522–546.
[6] G. Monegato, Singular Integral equations in the design of innovative airplane wing configurations, Rend. Semin. Mat. Univ. Politec. Torino 76 (2) (2018) 151–163.
[7] P.K. Banerjee, R. Butterfield, Boundary Element Methods in Engineering Science, first ed., McGraw-Hill, Inc. River Edge, NJ, USA, 1981, p. 452.
[8] A. Aimi, M. Diligenti, G. Monegato, New numerical integration schemes for applications of Galerkin BEM to 2D problems, J. Numer. Methods Engrg. 40 (1997) 1977–1999.
[9] J.A. Cottrell, T.J.R. Hughes, Y. Bazilevs, Isogeometric Analysis: Toward Integration of CAD and FEA, John Wiley & Sons, 2009.
[10] G. Beer, B. Marussig, C. Dünser, The Isogeometric Boundary Element Method, Springer, 2020.
[11] M.A. Scott, R.N. Simpson, J.A. Evans, S. Lipton, S.P.A. Bordas, T.J.R. Hughes, T.W. Sederberg, Isogeometric boundary element analysis using unstructured T-splines, Comput. Methods Appl. Mech. Engrg. 254 (2013) 197–221.

[12] R.N. Simpson, M.A. Scott, M. Taus, D.C. Thomas, H. Lian, Acoustic isogeometric boundary element analysis, Comput. Methods Appl. Mech. Engrg. 269 (2014) 265–290.
[13] F. Calabrò, G. Loli, G. Sangalli, M. Tani, Quadrature rules in the isogeometric Galerkin method: State of the art and an introduction to weighted quadrature, in: Advanced Methods for Geometric Modeling and Numerical Simulation, Springer, 2019, pp. 43–55.
[14] M. Taus, G.J. Rodin, T.J.R. Hughes, M.A. Scott, Isogeometric boundary element methods and patch tests for linear elastic problems: Formulation, numerical integration, and applications, Comput. Methods Appl. Mech. Engrg. 357 (2019) 112591.
[15] M. Taus, G.J. Rodin, T.J.R. Hughes, Isogeometric analysis of boundary integral equations: High-order collocation methods for the singular and hyper-singular equations, Math. Models Methods Appl. Sci. 26 (8) (2016) 1447–1480.
[16] A. Buffa, R. Hiptmair, Galerkin boundary element methods for electromagnetic scattering, in: Topics in Computational Wave Propagation, Springer, 2003, pp. 83–124.
[17] G. Beer, C. Dünser, Isogeometric boundary element analysis of problems in potential flow, Comput. Methods Appl. Mech. Engrg. 347 (2019) 517–532.
[18] L.L. Chen, H. Lian, Z. Liu, H.B. Chen, E. Atroshchenko, S.P.A. Bordas, Structural shape optimization of three dimensional acoustic problems with isogeometric boundary element methods, Comput. Methods Appl. Mech. Engrg. 355 (2019) 926–951.
[19] J. Dölz, S. Kurz, S. Schöps, F. Wolf, Isogeometric boundary elements in electromagnetism: Rigorous analysis, fast methods, and examples, SIAM J. Sci. Comput. 41 (5) (2019) B983–B1010.
[20] Y. Gong, C. Dong, F. Qin, G. Hattori, J. Trevelyan, Hybrid nearly singular integration for three-dimensional isogeometric boundary element analysis of coatings and other thin structures, Comput. Methods Appl. Mech. Engrg. 367 (2020) 113099.
[21] B.H. Nguyen, X. Zhuang, P. Wriggers, T. Rabczuk, M.E. Mear, H.D. Tran, Isogeometric symmetric Galerkin boundary element method for three-dimensional elasticity problems, Comput. Methods Appl. Mech. Engrg. 323 (2017) 132–150.
[22] R.N. Simpson, S.P.A. Bordas, J. Trevelyan, T. Rabczuk, A two-dimensional isogeometric boundary element method for elastostatic analysis, Comput. Methods Appl. Mech. Engrg. 209 (2012) 87–100.
[23] K.V. Kostas, M.M. Fyrillas, C.G. Politis, A.I. Ginnis, P.D. Kaklis, Shape optimization of conductive-media interfaces using an IGA-BEM solver, Comput. Methods Appl. Mech. Engrg. 340 (2018) 600–614.
[24] Z. An, T. Yu, T.Q. Bui, C. Wang, N.A. Trinh, Implementation of isogeometric boundary element method for 2-D steady heat transfer analysis, Adv. Eng. Softw. 116 (2018) 36–49.
[25] A. Aimi, M. Diligenti, M.L. Sampoli, A. Sestini, Isogeometric analysis and symmetric Galerkin BEM: a 2D numerical study, Appl. Math. Comput. 272 (2016) 173–186.
[26] A. Aimi, F. Calabrò, M. Diligenti, M.L. Sampoli, G. Sangalli, A. Sestini, Efficient assembly based on b-spline tailored quadrature rules for the IgA-SGBEM, Comput. Methods Appl. Mech. Engrg. 331 (2018) 327–342.
[27] F. Calabrò, A. Falini, M.L. Sampoli, A. Sestini, Efficient quadrature rules based on spline quasi-interpolation for application to IgA-BEMs, J. Comput. Appl. Math. 338 (2018) 153–167.
[28] A. Falini, C. Giannelli, T. Kanduč, M.L. Sampoli, A. Sestini, An adaptive IgA-BEM with hierarchical B-splines based on quasi-interpolation quadrature schemes, Internat. J. Numer. Methods Engrg. 117 (10) (2019) 1038–1058.
[29] J.A. Cottrell, T.J.R. Hughes, A. Reali, Studies of refinement and continuity in isogeometric structural analysis, Comput. Methods Appl. Mech. Engrg. 196 (41–44) (2007) 4160–4183.
[30] R. Vázquez, A. Buffa, L. Di Rienzo, NURBS-based BEM implementation of high-order surface impedance boundary conditions, IEEE Trans. Magn. 48 (12) (2012) 4757–4766.
[31] L. Beirao Da Veiga, A. Buffa, G. Sangalli, R. Vázquez, Mathematical analysis of variational isogeometric methods, Acta Numer. 23 (2014) 157–287.
[32] W.L. Wendland, E.P. Stephan, A hypersingular boundary integral method for two-dimensional screen and crack problems, Arch. Ration. Mech. Anal. 112 (4) (1990) 363–390.
[33] V.J. Ervin, R. Kieser, W.L. Wendland, Numerical approximation of the solution for a model 2-D hypersingular integral equation, in: Computational Engineering with Boundary Elements, Computational Mechanics Publications, Southampton, 1990, pp. 85–99.
[34] J.C. Nedelec, Integral equations with non integrable kernels, Integral Equations Operator Theory 5 (1) (1982) 562–572.
[35] Y.P. Gong, C.Y. Dong, Y. Bai, Evaluation of nearly singular integrals in isogeometric boundary element method, Eng. Anal. Bound. Elem. 75 (2017) 21–35.
[36] S. Keuchel, N.C. Hagelstein, O. Zaleski, O. von Estorff, Evaluation of hypersingular and nearly singular integrals in the isogeometric boundary element method for acoustics, Comput. Methods Appl. Mech. Engrg. 325 (2017) 488–504.
[37] M. Feischl, G. Gantner, A. Haberl, D. Praetorius, Optimal convergence for adaptive IGA boundary element methods for weakly-singular integral equations, Numer. Math. 136 (2017) 147–182.
[38] K. Mørken, Some identities for products and degree raising of splines, Constr. Approx. 7 (1991) 195–208.
[39] T. Lyche, L. Schumaker, Local splines approximation methods, J. Approx. Theory 15 (1975) 294–325.
[40] C. Manni, F. Pelosi, M.L. Sampoli, Quasi–interpolation in isogeometric analysis based on generalized B–splines, CAGD 27 (2010) 656–668.
[41] F. Mazzia, A. Sestini, The BS class of Hermite spline quasi-interpolants on nonuniform knot distributions, BIT 49 (3) (2009) 611–628.
[42] F. Mazzia, A. Sestini, Quadrature formulas descending from BS Hermite spline quasi-interpolation, J. Comput. Appl. Math. 236 (2012) 4105–4118.
[43] J. Dölz, H. Harbrecht, S. Kurz, S. Schöps, F. Wolf, A fast isogeometric BEM for the three dimensional Laplace and Helmholtz problems, Comput. Methods Appl. Mech. Engrg. 330 (2018) 83–101.
[44] J. Dölz, H. Harbrecht, S. Kurz, M. Multerer, S. Schöps, F. Wolf, Bembel: The fast isogeometric boundary element C++ library for Laplace, Helmholtz, and electric wave equation, SoftwareX 11 (2020) 100476.

[45] C. Schwab, W.L. Wendland, Kernel properties and representations of boundary integral operators, Math. Nachr. 156 (1992) 156–218.
[46] S.A. Sauter, C. Schwab, Boundary Element Methods, Springer Series in Computational Mathematics, vol. 39, Springer-Verlag, Berlin, Heidelberg, 2011.
[47] A. Aimi, M. Diligenti, G. Monegato, Numerical Integration schemes for the BEM solution of hypersingular integral equations, J. Numer. Methods Engrg. 45 (1999) 1807–1830.
[48] E.P. Stephan, W.L. Wendland, An augmented Galerkin procedure for the boundary integral method applied to two-dimensional screen and crack problems, Appl. Anal. 18 (3) (1984) 183–219.
[49] G. Farin, J. Hoschek, M.S. Kim, Handbook of Computer Aided Geometric Design, Elsevier, 2002.
[50] J. Hoschek, D. Lasser, Fundamentals of Computer Aided Geometric Design, A. K. Peters, Ltd., 1996.
[51] K.E. Atkinson, The Numerical Solution of Integral Equations of the Second Kind, Cambridge University Press, 2009.
[52] G. Monegato, Numerical evaluation of hypersingular integrals, J. Comput. Appl. Math. 50 (1–3) (1994) 9–31.
[53] G. Monegato, Definitions, properties and applications of finite-part integrals, J. Comput. Appl. Math. 229 (2009) 425–439.
[54] S. Holzer, How to deal with hypersingular integrals in the symmetric BEM, Commun. Numer. Methods. Eng. 9 (3) (1993) 219–232.
[55] A. Falini, T. Kanduč, A study on spline quasi-interpolation based quadrature rules for the isogeometric Galerkin BEM, in: C. Giannelli, H. Speleers (Eds.), Advanced Methods for Geometric Modeling and Numerical Simulation, in: Springer INdAM Series, vol. 5, Springer, 2019, pp. 193–227.
[56] A.P. Orsi, A note on spline approximation for Hadamard finite-part integrals, J. Comput. Appl. Math. 79 (1997) 67–73.
[57] L. Piegl, W. Tiller, The NURBS Book, second ed., in: Monographs in Visual Communication, Springer, USA, 2005.
[58] F.V. Postell, E.P. Stephan, On the h-, p-and hp versions of the boundary element method—numerical results, Comput. Methods Appl. Mech. Engrg. 83 (1) (1990) 69–89.
[59] A. Falini, T. Kanduč, M.L. Sampoli, A. Sestini, Cubature rules based on bivariate spline quasi-interpolation for weakly singular integrals, in: G. Fasshauer, M. Neamtu, L.L. Schumaker (Eds.), Approximation Theory XVI: Nashville 2019, Springer, 2020.